Csillagászati és Földtudományi Kutatóközpont
Földtani és Geokémiai Intézet

1121 Budapest, Budaörsi út 45. Tel.: (+36) 1 391-3137 www.csfk.org

Kutatási jelentés a Csillagászati és Földtani Kutatóintézet (CSFK) által a Pilisben végzett mintavételezési munkákról (2019.03-2020.05)

Felelős kutatásvezető: Dr. Demény Attila, CSFK FGI igazgató
A mintázásokat végzi: Kovács Richard és Berentés Ágnes
A jelentést készítette: Berentés Ágnes, Dr. Czuppon György tudományos főmunkatárs és Prof. Dr. Demény Attila igazgató

2021. február 15.

Dr. Demény Attila
igazgató, az MTA rendes tagja

Csillagászati és Földtani és Geokémiai Intézet * CSFK * Földtudományi Kutatóközpont

1) Bevezetés

2019. márciusában az Ariadne-barlangrendszer és az Ajándék-barlang klimatológiai, légkörzési, valamint beszivárgási és cseppkőképződési mechanizmusainak megismerésére irányulóan mintavételezések és monitoring vizsgálatok kezdődtek.
2020-ban a monitoring vizsgálatok az Ajándék- és a Vacska-barlangokra koncentrálódtak. Ezutóbbi esetében a korábban megkezdett vizsgálatok mikrobiológiai mintavételezéssel egészültek ki.

2) CO_2 monitoring

A barlangi CO_2 elsősorban a talaj mikrobiológiai aktivitásából ered. A talajon keresztülfolyó, CO_2-től enyhén savas csapadékvíz beszivárog a kőzetek repedéseibe, oldja azt. A nyomás növekedésével az oldóképesség is nő, majd ha a vízcsepp nagyobb légtérbe érkezik a lecsökkenő nyomás hatására elillan a CO_2 egy része és kiválik a karbonát (cseppkőképződés). Ennek jelenléte és mértéke nem csak a cseppkövek képződésében, de azok visszaoldásában is szerepet játszhat, amennyiben túlzottan magas a gáz mennyisége. A barlangi CO_2 mennyiségét befolyásolja a szellőzöttség és légáramlási viszonyok, így a külső hőmérséklet is. Ebből következően ez az érték évszakos változást mutat. Még a felszínen 320-450 ppm közötti CO_2 értékek az általánosak, addig a barlangjáratban ez 1500-4500 ppm. Az Ariadne-barlangrendszer cseppkőképződésének jobb megismerése érdekében a rendszer egyik tagjába, a Vacska-barlang Mérföldkőháti-termében elhelyeztünk egy CO_2 mérő és regisztráló műszert, melyet a STIEBER Levegőtisztaság-védelmi Bt.-től bérel az intézet. A műszer jelenleg is 2 óránként 7 percen keresztül működik, 2 perces időközökkel rögzíti az aktuális CO_2 értékeket(ppm-ben). A most már több, mint 1,5 éves detektálási adatsoron szemléltetve jól látszik, hogy júniusban, a detektálás kezdetekor mért 0,6 tszf%-os érték (6000 ppm) ősszel, tovább növekedett a barlangban (elérve a 9000 ppm-t). Majd, a külső hőmérséklet csökkenésével a barlangi légkörzés megfordult (a Vacska-barlang bejáratán keresztül befelé áramlik a levegő, ha a barlang átlagos hőmérséklet magasabb, mint a felszínen mért hőmérséklet). Ebben az esetben a beáramló levegő felhígítja, átszellőzteti a barlangot, jelentős visszaesést okozva a CO_2 koncentrációjában *(1. ábra)*. A külső hőmérséklet növekedésével a CO_2 szintje is ismét emelkedni fog. A mellékelt diagramm szépen szemlélteti ezt az évszakosságot.
Terepi megfigyelés alapján, az erős szél szintén hirtelen változást okozhat a barlangi légkörzésben, ezáltal a CO_2 mennyiségben is. A Leány-, és Legény-barlang nagyméretű bejáratán át befújó szél a rendszer többi tagjának légkörzését is megfordíthatja.

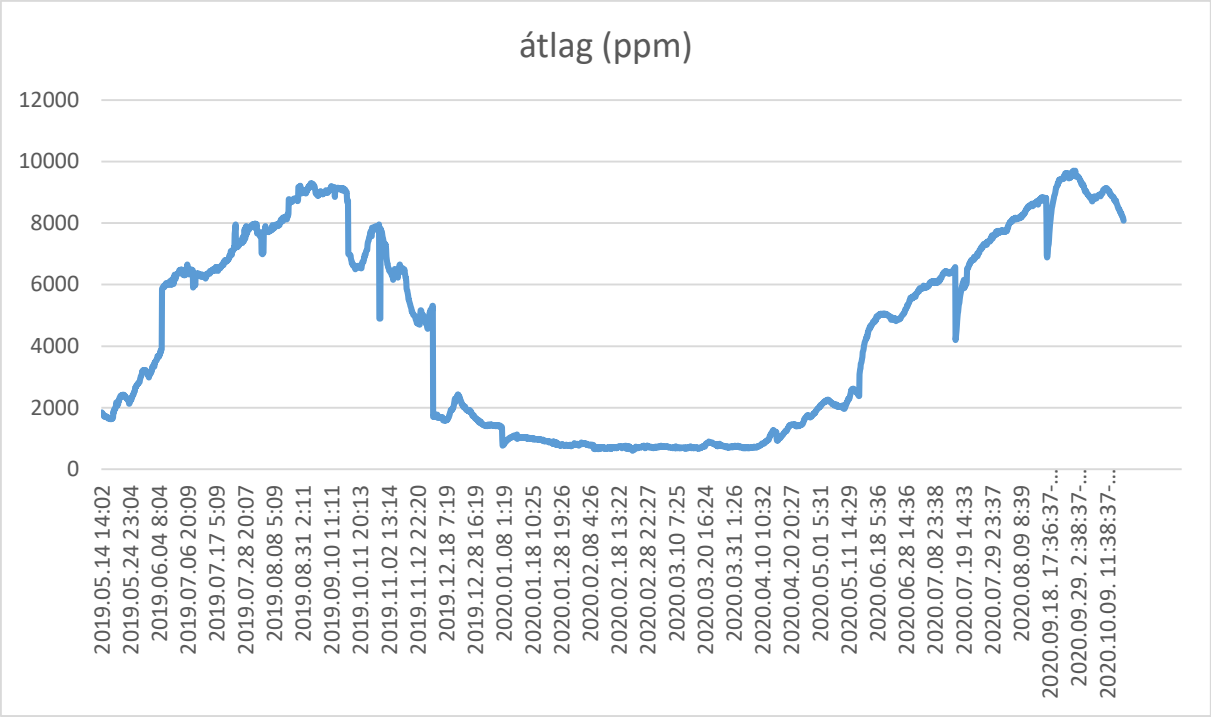

1. *ábra: A CO_2 koncentráció értékek változása 2019 májustól 2020 októberéig terjedő időszakban, a Vacska-barlangban.*

2. Csepegővíz- és karbonát kiválás gyűjtése

Ennek keretében a kőzetrétegen át barlangba beszivárgó csepegővizekből gyűjtünk mintát, kihelyezett mintavevő kannákba, vagy közvetlenül a cseppkövekről gyűjtjük be eppendorf csövekbe a cseppeket. A kannákba gyűjtött csepegések intenzitását eddigiekben a Rózsát-teremben kihelyezett intenzitásmérő műszerrel rögzítjük. 2021 januárjában a mintagyűjtési pontot áthelyeztük a Cseppköves-hasadékba, egyrészt, hogy olyan helyről gyűjtsünk, ahol kevésbé érvényesül a barlangi légkörzés, másrészt, hogy a korábban innen gyűjtött **V_03** mintaszámú cseppkő képződési körülményeiről tudhassunk meg többet **(2. ábra).**
A Rózsát-teremben korábban további 5 csepegési pont alá kihelyezett üveglapokat továbbra is kint hagytuk **(3-4. ábra).** A kéthavonta begyűjtött üveglapokból kettő megy mikrobiológiai vizsgálatokra, a többin a „frissen" kivált karbonát nyomelem- és stabilizotóp összetétele kerül meghatározásra.
Ezek segíthetnek a karbonát kiválás során végbemenő folyamatok (frakcionáció) jellemzésében, és ezáltal a cseppkövekben tapasztalt nyomelem és izotóp-összetétel értelmezésében.

2. ábra: A Cseppköves-hasadékba helyezett csepegés-mintagyűjtő és az intenzitásmérő logger.

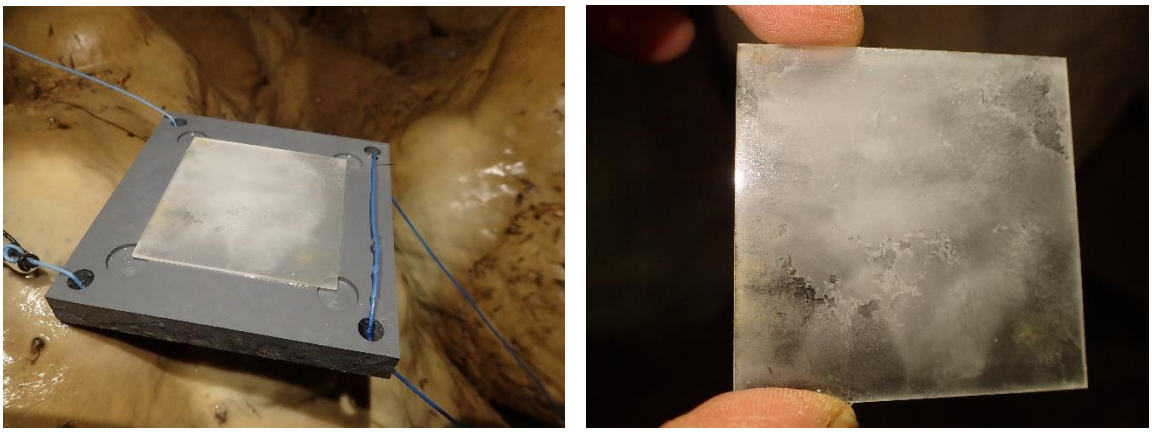

3-4. ábra: karbonátkiválás a kihelyezett üveglapokon

3. **Vízszint regisztrálás az Ajándék-barlang tavaiban** (írta: Fekete Zsombor és Berentés Ágnes)

Az Ajándék-barlang egyik különlegessége a 2014-ben felfedezett három tó, amelyek 1 km hosszú járatrészt töltenek ki. A három különálló tó vízszintje a csapadékutánpótlást lassan követve változik (lassú csökkenés, és gyors emelkedés jellemzi). Viszont a két tó vízszintje mind csökkenés, mind növekedés esetén 40 cm eltéréssel követik egymás változásait.

Mindhárom tóba automata vízszintregisztrálókat telepítettünk. A telepítés az első és második tóba 2019.07.11-én, a harmadik tóba 2019.10.08-án történt. Két alkalommal történt kiolvasás, mindkét alkalommal lentebb kellett helyezni a nyomásmérő szondát, mivel a vízszint csökkenése következtében hamarosan szárazra került volna. A harmadik tó vízszintje viszonylag hamar, 2019. december 11-én, a járható, hozzáférhető szakasz alá csökkent. A rögzített vízszintcsökkenés egy majdnem lineáris folyamatot mutat. Megjegyezhető, hogy ebben az időszakban a másik két tó csökkenése is majdnem lineáris volt. Az egyes és kettes tóban szerencsére 2019. júliusban sikerült egy nagyon rövid emelkedő szakaszt is rögzíteni. Ez Először a 2-es, majd az 1-es tóban július vége – augusztus körül megállt és csökkenni kezdett. A két tó vízszintje azonos sebességgel csökkent és lineáris jelleget mutatott egészen 2020 márciusig, amikor lecsökkent a vízszint változás sebessége (váll-szerűen). Egy átmeneti időszak után pedig újra lineáris változás állt be. A két görbe itt szintén párhuzamos, tehát a két tó vízszintváltozás sebessége azonos, a korábbi lineáris meredekséggel viszont nem azonos, megközelítőleg fele akkora meredekség alakult ki. A hőmérséklet az 1-es tó esetében egy nagyon lassú melegedést mutat, 8.05°C-ról 8.2°C-ra, ami az eszköz mérési pontosságát éppen csak meghaladja. A 2-es tó esetében teljes mértékben változatlan a víz hőmérséklete. Az elektromos vezetőképességben szintén minimális, mérési pontosság közeli változásokat észleltünk. Az 1-es tó esetében, a 2020 márciusi „jellegváltozás” előtt valamivel megnőtt (10 µS/cm körüli értékkel) a vezetőképesség. Miután a hőmérséklet is az 1-es tó mérési pontjában mutatott egy minimális változás, feltételezhető, hogy ez a mérési pont a tavak táplálásához közelebb van, mint a 2-es tó mérési pontja.

A vízszint időbeli változása egy nagyon kiegyenlített jelleget mutat, amire látszólag a felszínen megszokott éves periódus nincs hatással. Több éves periódusok jellemezhetik, amiből még csak a csökkenő ág egy részét és egy nagyon rövid emelkedő szakaszt sikerült megmérni. A méréseket érdemes több éves időtartamra tervezni. A vízszintregisztrálókat célszerű hosszabb légzőkábellel rendelkező eszközre cserélni és a cserét az alacsony vízállás mellett megoldani.

4. ábra: Dataqua kiolvasás alacsony vízszintnél, a 2. tó lejáratánál.

5. Mikrobiológiai vizsgálatok (írta: Lange-Enyedi Nóra Tünde)

A Vacska-barlangban folytatott geokémiai monitoring jellegű kutatást 2020-ban mikrobiológiai vizsgálatokkal egészítettük ki, hiszen a barlangban ezidáig nem történt vizsgálat a mikrobiális diverzitás széleskörű feltárására. A baktériumközösségek összetételének időbeli változását és a biogeokémiai folyamatokban való részvételét szeretnénk tanulmányozni. Célunk a Vacska-barlangban a mikrobiális tevékenység és a karbonátképződés összefüggéseinek feltárása, amit korábbi barlangi kutatások során sikerült kimutatni (Enyedi et al., 2020).

Eredmények

Az eddigi mintavételekre 2020 júniusában és szeptemberében került sor. Berentés Ágnes vett mintákat a barlang feletti talajból, illetve a Rózsát-teremből, a Mérföldkőháti-teremből, a Cseppköves hasadékból és a Fennkőháti-teremből a cseppkőfelszínekről és barlangi talajból (1. táblázat). A mintavétel a cseppkőfelszínekről steril fiziológiai sóoldatba mosott steril vattapálcikákkal történt, míg a begyűjtött üveglemezekről a kiválást laboratóriumban gázégő lángja mellett aszeptikus módon steril spatulával.

1. táblázat: A Vacska-barlangból (Va) 2020-ban mikrobiológiai vizsgálatok céljára vett minták.

Minta típus	**Mintajelzés**	**Időpont**
Felszíni talajminta (T)	VaT	2020.06.11.
	VaT2	2020.09.17.
Rózsát-terem (R)		
főcsepegési ponttal szembeni üveglemez (a)	VaR2a (elhelyezés után 2 hónap elteltével)	2020.06.11.
üveglemezes minta (b)	VaR2b (elhelyezés után 2 hónap elteltével)	2020.06.11.
	VaR3b (elhelyezés után 3 hét elteltével)	2020.09.17.
főcsepegés alatti cseppkőről (D) kenet	VaRD	2020.06.11.
	VaRD3	2020.09.17.
talaj (S)	VaRS	2020.06.11.
Mérföldkőháti-terem (M)		
talaj (S)	VaMS	2020.06.11.
Cseppköves hasadék (C)		
cseppkőfal (M)	VaCM	2020.06.11.
talaj (S)	VaCS	2020.06.11.
Fennkőháti-terem (F)		
pocsolya melletti aktív cseppkő (D)	VaFD	2020.06.11.
	VaFD2	2020.09.17.
talaj (S)	VaFS	2020.09.17.

A bakteriális közösség elemzését a mintákból kivont közösségi DNS 16S rRNS-gén V3-V4 régiójának új-generációs bázissorrend meghatározásával (Illumina MiSeq platformon, Michigan State University) végeztük (Tóth et al., 2020). A bioinformatikai kiértékelés (mothur v1.44.3) során minőségi szűrést végeztünk, kiszűrtük az amplifikációs és szekvenálási hibákat,

a kiméra szekvenciákat és a szingleton szekvenciákat (Schloss et al., 2009). A szekvenciák illesztése az SILVA Release138 SSU NR referencia adatbázis segítségével történt (Quast et al., 2013). Az OTU-k (operatív taxonómiai egységek) megállapítása 97%-os szekvencia hasonlósági küszöbnél történt (Tindall et al., 2010). A sikeresen megvizsgált mintákat tartalmazza az 1. táblázat.

A különböző minták baktériumközösségének elemzése során kapott eredmények mennyiségi jellemzőit a 2. táblázat foglalja össze.

2. táblázat: A 16S rRNS-gén amplikon szekvenálással kapott bakteriális OTU számok és diverzitás indexek. Az indexek esetében ábrázolt értékek az adathalmaz újramintavételezésének átlagértékei 14350 (Bacteria) és 2009 (Archaea) szekvencia alapján. A lefedettség értékek a Good-féle lefedettség becslő index alapján lettek számítva.

Minta	Csoport	Szekvenciaszám	OTU szám	Lefedettség	Shannon-index	Inverz Simpson-index
VaCM	Bacteria	20833	1119	98,71%	5,17	36,8
	Archaea	17314	76	98,50%	2,01	3,98
VaCS	Bacteria	26467	1323	97,37%	5,28	55,4
	Archaea	21561	85	98,15%	2,32	5,30
VaFD	Bacteria	30830	407	99,21%	2,96	7,81
	Archaea	14147	26	99,57%	0,45	1,17
VaFD2	Bacteria	28231	1563	96,64%	5,51	49,2
	Archaea	34216	74	98,38%	2,47	7,28
VaFS	Bacteria	22646	1055	98,51%	5,10	49,3
	Archaea	27225	126	97,21%	2,92	9,13
VaMS	Bacteria	25251	754	98,78%	4,12	13,6
	Archaea	49007	88	98,07%	2,46	5,52
VaR2a	Bacteria	29549	762	98,40%	4,52	28,8
	Archaea	2940	54	99,52%	2,43	6,82
VaR2b	Bacteria	33608	756	98,16%	4,14	18,9
	Archaea	2009	28	99,95%	1,82	3,23
VaRD	Bacteria	26753	1844	95,75%	5,73	72,0
	Archaea	8927	31	99,38%	0,88	1,63
VaRS	Bacteria	20792	1075	98,74%	5,33	62,1
	Archaea	14468	89	98,24%	2,52	5,18
VaRD3	Bacteria	26201	1426	96,69%	4,63	20,7
	Archaea	3675	42	99,56%	1,64	3,13
VaR3b	Bacteria	35267	713	98,13%	3,72	13,3
	Archaea	6388	50	99,21%	2,39	7,19
VaT	Bacteria	20034	3342	94,25%	7,06	263
	Archaea	10436	22	99,55%	1,73	4,61
VaT2	Bacteria	14350	2586	99,99%	7,11	434
	Archaea	8269	14	99,76%	1,65	4,41

Az előzetes eredmények alapján a szekvenciák száma megfelelő lefedettséget adott a bakteriális diverzitás feltárásához. A Bacteria doménbe tartozó baktériumok esetében a

diverzitás fokozatosan nőtt az üveglemezekről eltávolított biofilmektől kezdve, amit a cseppkövek felszíne, majd a barlangi talajminták és a felszíni talajminták követték, utóbbiban nagy mennyiségű 5%-nál is kevesebb relatív abundanciájú szekvenciával rendelkező baktériumok jelenlétére következtethetünk (5.C ábra). A barlangi és felszíni talajokban a legváltozatosabb anyagcserével jellemezhető baktériumok lehetnek jelen. Az Archaea doménbe tartozó baktériumok (ősbaktériumok) esetén azonban ez megfordul és a cseppkőfelszíni és a felszíni talaj baktériumközösségek bizonyultak a legkevésbé diverznek, amiket az üveglemezeket borító, majd a barlangi talajban élő baktériumközösségek követnek (2. táblázat).

Ehhez hasonlóan jelentős különbség látható a minták (üveglemezek, cseppkövek, talajok) közösségi összetételében (5-6. ábra) is. Számos OTU ismeretlen nemzetség vagy magasabb rendszertani kategória képviselője. Megfigyelhető bizonyos nemzetségek dominanciája a különböző termekből különböző időpontban vett minták baktériumközösségében. A legtöbb azonosított Bacteria doménbe tartozó nemzetség ismert képviselői aerob kemoorgano-heterotróf, köztük komplex szerves anyagok (kitin, cellulóz, lignin) lebontására képes baktériumok. A barlangokban gyakran előforduló, viszonylag alacsony szerves anyag tartalom miatt megjelenő kemolitotróf autotróf baktériumok és ősbaktériumok is jelen vannak, melyek képesek a barlangi környezetben nitrogén-körforgalom fenntartására és a biofilmek alapját képezik. A kialakuló biofilmek a barlangi tápláléklánc bázisát is adhatják. A különböző teremből vett minták közül a bejárathoz közelebbi Rózsát-teremben viszonylag több heterotróf baktériumot mutattunk ki, mint a barlang távolabbi részeiről, ahol az autotrófia dominál. Az üveglemezekről eltávolított biofilmek közösségei különböznek mintavételi hely és mintavételi időpont alapján. Több kimutatott nemzetség közel rokonai képesek a karbonátok kiválását indukálni laboratóriumi kísérletekben. A baktériumok megtapadását és a baktériumközösségek összetételét meghatározhatja a különféle minták ásványi összetétele.

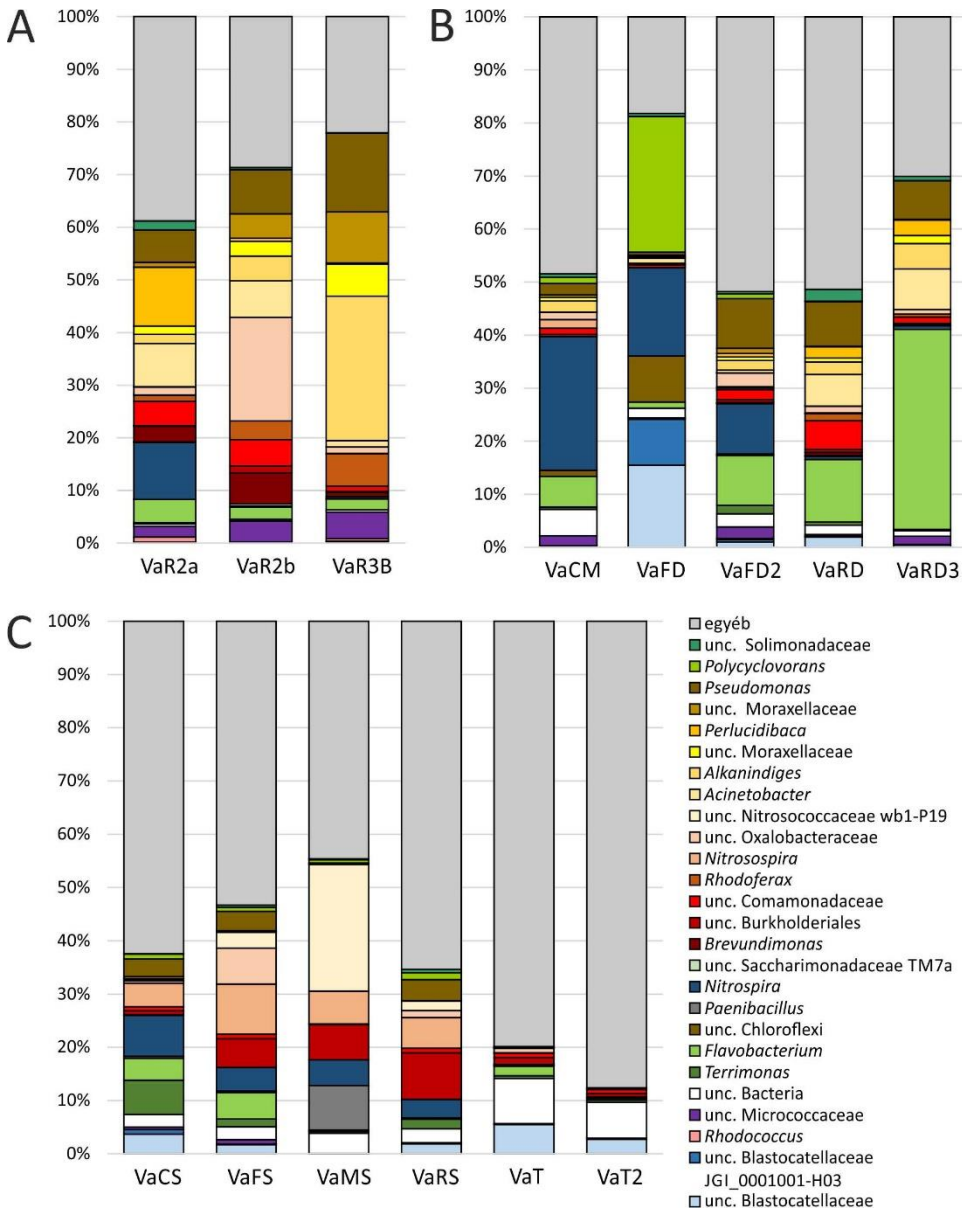

5. ábra: A Vacska-barlangból vett üveglemez (A), cseppkő (B) és talaj (C) minták bakteriális közösségének összetétele (Bacteria domén) filogenetikai nemzetség szinten. Az ábrán az 5% alatti relatív abundanciával rendelkező nemzetségek az egyéb kategóriába kerültek.

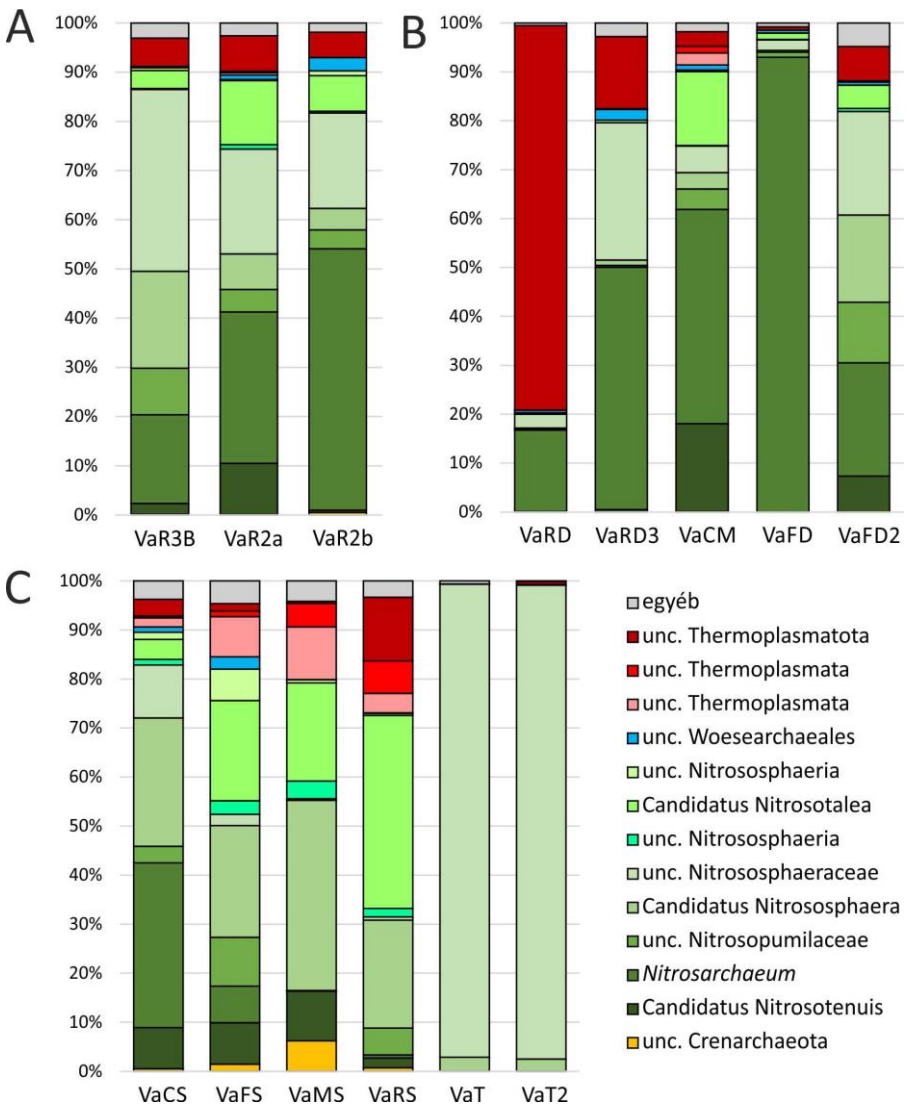

6. ábra: A Vacska-barlangból vett üveglemez (A), cseppkő (B) és talaj (C) minták bakteriális közösségének összetétele (Archaea domén) filogenetikai nemzetség szinten. Az ábrán az 5% alatti relatív abundanciával rendelkező nemzetségek az egyéb kategóriába kerültek.

6. A csepegővizek stabilizotóp és kémiai összetétele

A csepegővíz-mintagyűjtés a Vacska-barlangra koncentrálódott, ahol hat helyszínen történt mintavétel kétheti rendszerességgel. A különböző helyszínekről vett vízminták stabilizotóp-összetétele alapján megállapítható, hogy a Rózsát-terem markánsan elkülönül a többi vizsgált ponttól (Mérföldkőháti-terem, Cseppköves-terem, Nyeregponti-terem, Fennkőháti-terem), a hidrogén- és az oxigénizotóp-összetétele azoknál jóval pozitívabb értéket mutat (7. ábra). A Rózsát-teremben mért értékek közelebb esnek a csapadék éves, mennyiséggel súlyozott értékéhez, amely alapján arra lehet következtetni, hogy ezen a helyszínen „egyenletesebb” a beszivárgás, míg a többi helyszín esetében jóval nagyobb a téli csapadék hozzájárulása a csepegővízhez. Ez a különbség nagy valószínűséggel a beszivárgás módjával és a víz tartózkodási idejével van összefüggésben. A mért kémiai paraméterek közül különösen a Sr koncentráció és az abban tapasztalt különbség, jelezhet eltérő tartózkodási időt. A Rózsát-terem esetében a Sr koncentráció jóval alacsonyabb a többi teremhez képest (8. ábra), amely rövidebb tartózkodási időt valószínűsít (Czuppon et al., revised).

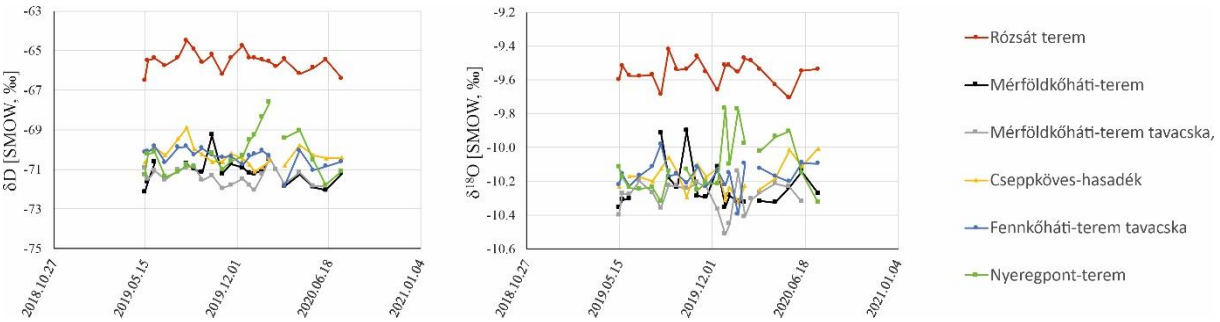

7. ábra: A Vacska-barlang csepegővizeinek hidrogén- (δD) és oxigénizotóp-összetétele $\delta^{18}O$).

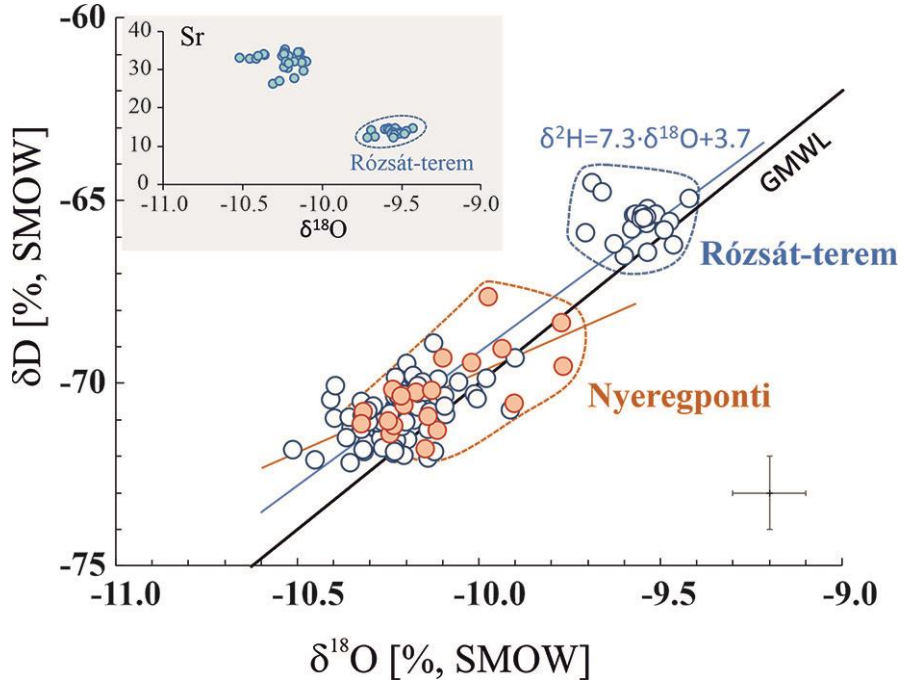

8. ábra: A Vacska-barlang csepegővizeiben mért oxigén és hidrogénizotóp-összetétel, valamint Sr koncentráció.

7. Cseppkőkutatás

• Az Ajándék-barlangból a korábbi évtizedek során történt törmelékgyűjtésből származó gyűjteményi cseppkő (AJ-1) stabilizotópos elemzését végeztük el. A karbonát szén- és oxigénizotópos mérése mellett a fluidumzárványokba zárt víz hidrogén- és oxigénizotópos elemzése is megtörtént. A cseppkövet 8 U-Th sorozatos korméréssel datáltuk, ami 240-180 ezer évvel ezelőtti képződést jelez. Az elemzések alapján a megadott időszakra paleohőmérsékletet számoltunk. Az eredmények a Chemical Geology folyóiratban jelentek

meg (Demény et al., 2021), a Nemzeti Park támogatásának megjelölésével. A cikk a jelen jelentéshez csatolva található.

- A Vacska-barlangban történt gyűjtésből származó cseppkövek (lásd a 2019-ről szóló jelentést) közül az előzetes kormérések alapján két cseppkő esetében készült részletes korvizsgálat. A V_01 jelű cseppkőből 10 AMS ^{14}C kormérést végeztünk az Atommagkutató Intézetben. Az adatok kiértékelése és a kormodell készítése jelenleg folyamatban van. A koradatok modellezése alapján a felső, mintegy 1,6 cm vastag rész az utolsó 1000 évet fedi le, az alatta levő mintegy 2 cm-es vastagságú réteg kb. 5500-6000 évvel ezelőtt képződött. A fiatalabb szakasz stabilizotóp-összetételei jól összevethetőek a független klimatológiai adatokkal, ami segít az idősebb cseppkövek adatainak értelmezésében.

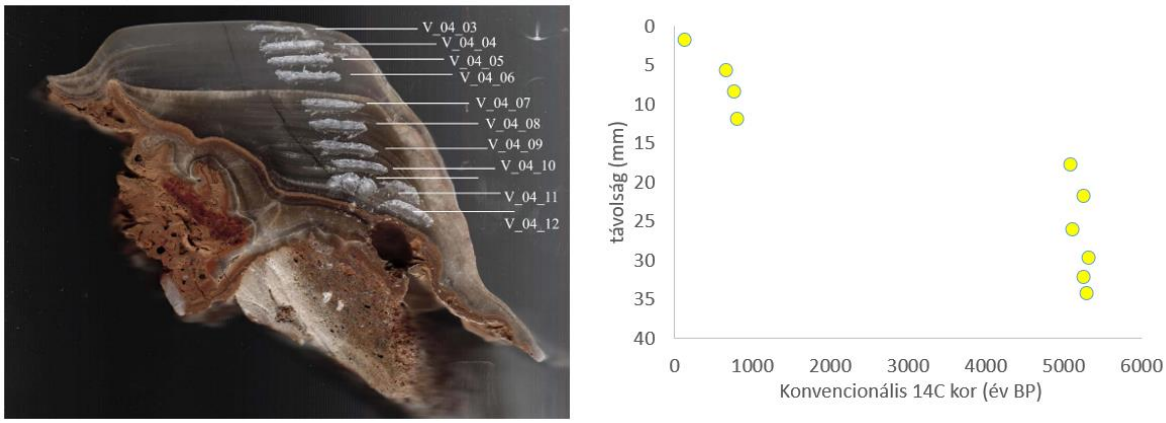

9. ábra. A V_01 cseppkő nem korrigált ^{14}C-koradatai.

A V_03 jelű cseppkőből 12 db. U-Th sorozatok kormérés és 20 db. AMS ^{14}C-elemzés készült. Az eredmények azt mutatják, hogy a cseppkő mintegy 10 ezer évvel ezelőtt kezdett növekedni és 8 ezer évvel ezelőtt állt le a növekedés. A cseppkő így a híres 8200 éves esemény jeleit rögzíti, amelynek részletes vizsgálata jelenleg folyik. A cseppkőből 175 db. C-O izotópelemzés, valamint 76 db. XRF Sr-tartalomelemzés készült. Az adatok a 8200 éves eseményt néhány éves felbontással mutatják. Az eredmények értelmezése és publikálása folyamatban van.

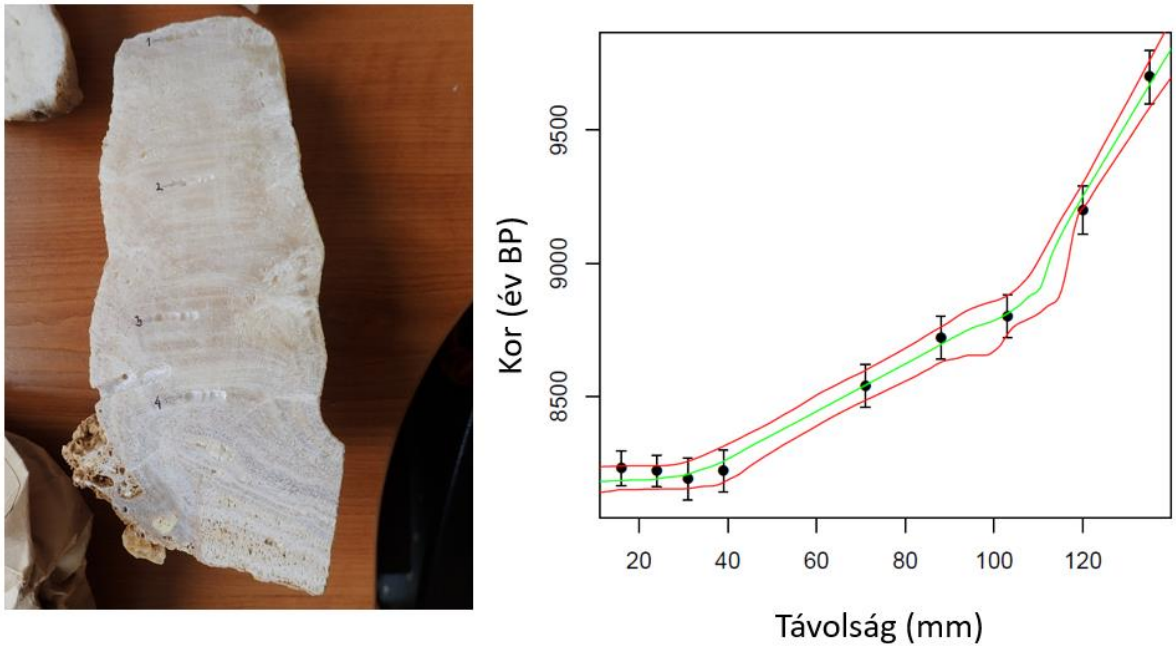

10. ábra. A V_03 cseppkő U-Th sorozatos koradatai és a StalAge kormodell.

Irodalomjegyzék

Czuppon Gy., Demény A., Leél-Őssy Sz., Stieber J., Óvári M., Dobossy P., Berentés Á., Kovács R. Monitoring and geochemical investigations of caves in Hungary: implications for climatological, hydrological and speleothem formation processes. In: Eds: Veress M., and Leél-Őssy Sz., Cave and Karst Systems of Hungary, Springer (revised).

Demény, A., Rinyu, L., Kern, Z., Hatvani, I.G., Czuppon, Gy., Surányi, G., Leél-Őssy, Sz., Shen., Ch.-Ch., Koltai, G. (2021): Paleotemperature reconstructions using speleothem fluid inclusion analyses from Hungary. Chemical Geology 563, 120051.

Enyedi, N. T., Makk, J., Kótai, L., Berényi, B., Klébert, S., Sebestyén, Z., Molnár, Z., Borsodi, A. K., Leél-Őssy, S., Demény, A., & Németh, P. (2020). Cave bacteria-induced amorphous calcium carbonate formation. *Scientific Reports*, *10*(1), 1–12.

Quast, C., Pruesse, E., Yilmaz, P., Gerken, J., Schweer, T., Yarza, P., Peplies, J., & Glöckner, F. O. (2013). The SILVA ribosomal RNA gene database project: Improved data processing and web-based tools. *Nucleic Acids Research*, *41*(D1), 590–596.

Schloss, P. D., Westcott, S. L., Ryabin, T., Hall, J. R., Hartmann, M., Hollister, E. B., Lesniewski, R. A., Oakley, B. B., Parks, D. H., Robinson, C. J., Sahl, J. W., Stres, B., Thallinger, G. G., Van Horn, D. J., & Weber, C. F. (2009). Introducing mothur: Open-source, platform-independent, community-supported software for describing and comparing microbial communities. *Applied and Environmental Microbiology*, *75*(23), 7537–7541.

Tindall, B. J., Rosselló-Móra, R., Busse, H. J., Ludwig, W., & Kämpfer, P. (2010). Notes on the characterization of prokaryote strains for taxonomic purposes. *International Journal of Systematic and Evolutionary Microbiology*, *60*(1), 249–266.

Tóth, E., Toumi, M., Farkas, R., Takáts, K., Somodi, C., & Ács. É. (2020). Insight into the hidden bacterial diversity of Lake Balaton, Hungary. *Biologia Futura*, *70,* 383–391.

A kutatás résztvevői: Lange-Enyedi Nóra Tünde, Makk Judit, Borsodi Andrea, Czuppon György, Németh Péter, Berentés Ágnes, Demény Attila

Chemical Geology 563 (2021) 120051

Contents lists available at ScienceDirect

Chemical Geology

journal homepage: www.elsevier.com/locate/chemgeo

Paleotemperature reconstructions using speleothem fluid inclusion analyses from Hungary

Attila Demény [a,*], László Rinyu [b], Zoltán Kern [a], István G. Hatvani [a], György Czuppon [a,b], Gergely Surányi [b,c], Szabolcs Leél-Őssy [d], Chuan-Chou Shen [e,f], Gabriella Koltai [g]

[a] Institute for Geological and Geochemical Research, Research Centre for Astronomy and Earth Sciences, Budaörsi út 45, Budapest H-1112, Hungary
[b] Isotope Climatology and Environmental Research Centre (ICER), Institute for Nuclear Research, Bem tér 18/c, Debrecen H-4026, Hungary
[c] MTA-ELTE Geological, Geophysical and Space Sciences Research Group, 1117 Budapest, Pázmány Péter s. 1/c, Hungary
[d] Department of Physical and Applied Geology, Eötvös Loránd University, Pázmány Péter sétány. 1/C, Budapest H-1117, Hungary
[e] High-Precision Mass Spectrometry and Environment Change Laboratory (HISPEC), Department of Geosciences, National Taiwan University, Taipei 10617, Taiwan, ROC
[f] Research Center for Future Earth, National Taiwan University, Taipei 10617, Taiwan, ROC
[g] Institut für Geologie, Leopold-Franzens-Universität Innsbruck, Austria

ARTICLE INFO

Editor: Michael E. Boettcher

Keywords:
Speleothem
Paleotemperature reconstruction
Fluid inclusion
Calcite
Stable isotope composition
Clumped isotope

ABSTRACT

The combined use of the stable isotope compositions of speleothem carbonate and inclusion-hosted water presents great potential in paleotemperature reconstructions, due to the various temperature-dependent isotope fractionations detected in cave systems and their environment. This paper evaluates the applicational possibilities of hydrogen and oxygen isotope measurements of inclusion-hosted water and its host calcite, in three different approaches: i) direct determination of calcite-water oxygen isotope fractionation by measuring inclusion water and carbonate compositions, ii) calculation of water oxygen isotope composition from hydrogen isotope data and of temperature from the inferred calcite-water fractionation, and iii) calculation of formation temperature from measured hydrogen isotope data and its temperature dependence in the modern precipitation water. Fluid inclusion oxygen and hydrogen isotope compositions as well as calcite oxygen isotope compositions were determined for five speleothem occurrences in Hungary. Although the background processes are not resolved, calculations involving measured calcite and water oxygen isotope compositions yielded unrealistic paleotemperatures, likely because of *syn*-formation isotope fractionation processes and diagenetic alterations. The hydrogen isotope data may yield realistic temperatures, provided that long-term isotopic composition - temperature relationships are known and the stable hydrogen isotope composition of the precipitation waters in the study area is temperature-controlled. Winter half-year and annual isotope-temperature relationships (δ^2H/T gradients) were calculated using multidecadal isotope composition records from the Global Network of Isotopes in Precipitation (GNIP), gridded surface temperatures, and precipitation amounts from the *E*-OBS 21.0e database. The calculations yielded a paleotemperature record for the last ~250 ka, with average precisions ranging from ±0.6 °C for interglacial to ±2.4 °C for glacial periods. Clumped isotope analyses of cave-hosted flowstones support the inferred formation temperatures based on gradients, while detection of kinetic fractionations by combined hydrogen and oxygen isotope analyses of calcite and inclusion water lead to filtering clumped isotope (Δ_{47}) data and more coherent Δ_{47}-temperature relationships.

1. Introduction

Stable isotope analyses of inclusion-hosted water extracted from speleothems began over 40 years ago (Schwarcz et al., 1976; Harmon and Schwarcz, 1981; Yonge, 1982). The application of laser absorption spectroscopy has given new momentum to the research field, as the technique is cost-effective compared to mass spectrometry and yields combined hydrogen and oxygen isotope compositions on the same H_2O aliquot, with precisions reaching or exceeding mass spectrometric analyses (Hodell et al., 2012; Arienzo et al., 2013; Affolter et al., 2014;

* Corresponding author.
E-mail address: demeny@geochem.hu (A. Demény).

https://doi.org/10.1016/j.chemgeo.2020.120051
Received 2 July 2020; Received in revised form 28 December 2020; Accepted 29 December 2020
Available online 9 January 2021

Czuppon et al., 2014; Demény et al., 2016a; Uemura et al., 2016; de Graaf et al., 2020). We note here that, although there are other isotopes of hydrogen and oxygen (radioactive ^{3}H and stable ^{17}O) besides ^{2}H, ^{1}H, ^{18}O, and ^{16}O, the term hydrogen and oxygen isotope composition is based on the abundances of the latter isotopes (expressed as $\delta^{2}H$ and $\delta^{18}O$, respectively) and will be used in this paper for simplicity's sake.

Combined analyses of hydrogen and oxygen isotope ratios performed directly on H_2O are particularly advantageous in the case of minerals whose chemical composition contains no hydrogen or oxygen (like fluorite, CaF_2) that would undergo isotope exchange with fluid inclusion water. Thus, they may provide direct information on the parent solution, without entrapment-related isotope fractionation (Czuppon et al., 2014). Contrary to oxygen-free minerals, late-stage oxygen isotope exchange is possible between inclusion-hosted water and the host carbonate (e.g., Uemura et al., 2020), so potential alteration processes must be evaluated. Analyses of stable isotope compositions of inclusion-hosted water, combined with the determination of the oxygen isotope composition of the host carbonate produce carbonate-water oxygen isotope fractionation values that in turn can be used to calculate formation temperatures, when fractionation-temperature relationships are applied (Schwarcz et al., 1976; Uemura et al., 2016). However, studies dealing with such analyses seldom use the measured carbonate and inclusion water oxygen isotope compositions to calculate formation temperatures (Allan et al., 2018). A potential reason may be the diagenetic alteration processes described by Demény et al. (2016a) that deteriorate the original oxygen isotope composition of the encapsulated water, due to post-entrapment fractionation processes. Recent experimental results suggest that simple isotopic exchange has only a minor influence on the oxygen isotope composition of inclusion-hosted water and on temperature reconstruction (Uemura et al., 2020). Extensive recrystallization or dissolution-reprecipitation of the host carbonate is therefore required to create significant oxygen isotope shifts. Alternatively, instrumental effects or isotope exchange processes related to analytical procedure may cause shifts away from the original oxygen isotope compositions (Meckler et al., 2015). Additionally, site-specific carbonate-water oxygen isotope fractionation may also complicate the interpretation of calculated temperatures. Various calcite-water oxygen isotope fractionation equations have been published in the last decades, depending on carbonate precipitation conditions and water chemistry (see Demény et al., 2017a; Daëron et al., 2019; Jautzy et al., 2020; and references therein). The uncertainty deriving from differences in these fractionation equations (up to about 8 °C using the most differing equations of Kim and O'Neil, 1997, and Daëron et al., 2019) affects all of the paleotemperature calculations that apply oxygen isotope compositions of calcite and water.

Another approach in fluid inclusion-based paleotemperature reconstruction is the use of the hydrogen isotope composition to calculate the water's oxygen isotope value (Zhang et al., 2008). In this method, the hydrogen isotope composition is determined for the extracted fluid inclusion, and the water oxygen isotope value is calculated using the local or global meteoric water line (GMWL, Craig, 1961, the relationship between hydrogen and oxygen isotope compositions of meteoric waters). As the water oxygen isotopic composition is calculated and the carbonate is measured, the formation temperature is given as above. This approach has two major uncertainties: i) knowing the local meteoric water line equation, which is valid in the time period studied; and ii) the selection of the carbonate-water oxygen isotope fractionation equation (see above).

The third approach is based solely on hydrogen isotope compositions and uses the composition-temperature relationship that was determined for the research area (Demény et al., 2017a, 2019; Affolter et al., 2019). The advantage of this method is that it relies on a relatively simple and robust analytical technique, whereas the disadvantages are that the composition-temperature relationship is estimated only from recent monitoring activities and that the approach can only be applied in settings where the hydrogen and oxygen isotope compositions of the precipitation water are driven by surface temperature. The latter requirement is not fulfilled in the maritime tropical-subtropical and Mediterranean regions, where the isotopic compositions of precipitation depend on the amount of rainfall.

This paper evaluates these three approaches using 156 fluid inclusion and associated calcite analyses from five speleothems collected in Hungary. The conventional isotope analyses were supplemented with clumped isotope measurements on speleothems that cover glacial-interglacial periods and, thus, a relatively large temperature range. We demonstrate that in a temperature-sensitive region, where the composition-temperature relationship is known from monitoring activities spanning several decades, hydrogen isotope compositions can be used in paleotemperature reconstructions.

2. Materials and Methods

2.1. Speleothems

Five speleothems from four caves were examined in this paper (see Fig. 1 and the Supplementary Material). Speleothems ZEP and BAR-II were collected from Baradla Cave (NE Hungary), while a flowstone core (BNT-2) was obtained from the nearby Béke Cave (NE Hungary). The Baradla and Béke caves are near the village of Jósvafő, and at their closest point, they are less than 1 km from each other. The ZEP (abbreviated from „Zeppelin") stalagmite, drilled from the bottom (see Supplementary Material, Fig. S1), is 7 m long, broken, and tilted. Inspections of the drill cores ZEP-1, −2, and − 3 revealed that the stalagmite was built on a ~ 40 cm thick flowstone layer, which is examined in this paper. The core material is primarily characterized by columnar calcite that contain elongated fluid inclusions aligned in growth direction (Fig. S2). U-Th dating of 15 samples (Table S1) revealed that the flowstone covers the period between ~330 and 150 ka BP (thousand years before present, where „present" refers to 1950 CE). An age-depth model was constructed for the inner part of the core covering a period of 227 to 159 ka BP (See Supplementary Material, Fig. S3). The ZEP-1 core was selected for detailed analyses. Both the BAR-II (Baradla Cave) and BNT-2 (Béke Cave) speleothems were analyzed in previous research. In this study, we refer to the original age models constructed for these two speleothems (Demény et al., 2017a and Demény et al., 2019, respectively). Previously published data on the water contents, the inclusion water $\delta^{2}H$ and $\delta^{18}O$ values, and the carbonate $\delta^{18}O$ values of stalagmite BAR-II (Demény et al., 2017a) are used. For BNT-2, however, new data on the isotopic ratios of speleothem fluid inclusions are reported in this paper. The Baradla and Béke caves were monitored from 2013 to 2016 (Czuppon et al., 2018). The long term cave air temperature in the Baradla Cave was 10.2 ± 0.3 °C, the drip water at a selected monitoring site had stable hydrogen and oxygen isotope compositions of −65 ± 2‰ and − 9.4 ± 0.3‰, respectively (n = 19). The nearby Béke Cave is characterized by similar values (9.8 ± 0.3 °C; −65 ± 1.5‰; −9.4 ± 0.2‰; n = 63). The temperature and stable isotope data showed no significant seasonal fluctuations (Czuppon et al., 2018).

The 33 cm long stalagmite AJ-1 was found on the cave floor in Ajándék Cave (North-Central Hungary). The stalagmite carbonate is primarily characterized by dendritic fabric, with layers of columnar calcite (Figs. S4A and B). Fluid inclusions are usually elongated and arranged in growth layers (Figs. S4C and D). Eight U-Th ages ranging from ~240 to ~180 ka BP were obtained for AJ-1 (Table S1). These were used to establish an age-depth model (Fig. S5). The Ajándék Cave was monitored from 2013 to 2016 that yielded mean cave air temperature and drip water stable hydrogen and oxygen isotope data (8.9 ± 0.7 °C; −71 ± 0.7‰; −10.2 ± 0.1‰, respectively; n = 38; Supplementary Table S2).

The fifth speleothem sample examined in this study is a flowstone from Abaliget Cave (Southern Hungary, Fig. 1), which was dated and analyzed for carbonate carbon and oxygen isotope compositions by Koltai et al. (2017). Two drill cores (ABA-1 and ABA-2) covering the

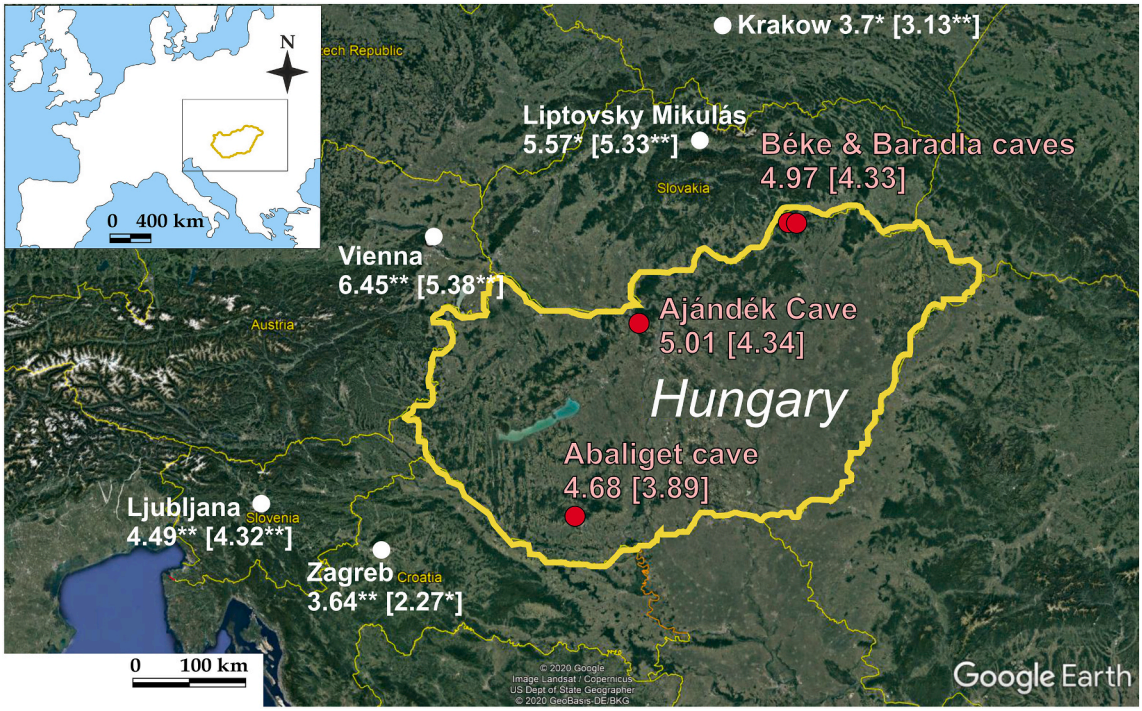

Fig. 1. Map of the study area, with the studied caves' locations and GNIP stations. Modern-day δ^2H/T gradient values (in ‰ °C–1) are also shown. δ^2H/T values for the winter half year (October–March) are followed by data obtained for the entire year (in square brackets). White dots and letters: GNIP stations. Red dots and pink letters: cave locations. Reference period: 1980–2018.The asterisks show significance level *: $p \leq 0.1$; **: $p \leq 0.05$. The values adjacent to the cave locations are the inverse distance weighted mean δ^2H/T slopes. Basemap source: Google Earth: Landsat/Copernicus imagery; accessed on 12.12.2020. (For interpretation of the references to colour in this figure legend, the reader is referred to the web version of this article.)

period of 165 to 105 ka BP (Koltai et al., 2017) were sampled for fluid inclusion analyses. Stable hydrogen and oxygen isotope values of drip water (−65.2‰ and 9.3‰, respectively; $n = 7$), collected from soda straws above the flowstone, were consistent with the local meteoric water line (Koltai et al., 2017). These drip water compositions are very close to those of the Baradla and Béke caves (see above) and are slightly lower than the amount weighted annual precipitation hydrogen and oxygen isotope values (−62.3‰ and 9.1‰, respectively; Czuppon et al., 2018). This difference indicates that the drip water is biased toward winter precipitation due to extensive evaporation during summer in the studied region. The drip water compositions of the Ajándék Cave are significantly lower (see above), approaching the amount weighted average winter precipitation hydrogen and oxygen isotope compositions (−71‰ and 10.2‰, respectively; Czuppon et al., 2018). In spite of the differences between the Ajándék Cave and the other caves, all of the studied caves showed stable conditions with no significant seasonal fluctuations. The drip water compositions described above are used in the paleotemperature calculations described below as modern-day values.

2.2. Stable isotope analyses

Stable oxygen isotope ratios of calcites (samples ZEP-1 and AJ-1) were measured using an automated GASBENCH II sample preparation device connected online in continuous flow mode to a Thermo Finnigan Delta Plus XP isotope ratio mass spectrometer at the Institute for Geological and Geochemical Research (IGGR in Budapest, Hungary). The isotopic compositions are expressed as $\delta^{18}O_{cc}$ values in ‰, relative to V-SMOW. The accuracies of $\delta^{18}O_{cc}$ values are better than ±0.1‰. Analytical details are described in Demény et al. (2019). Water contents and the stable hydrogen and oxygen isotope compositions of inclusion-hosted waters were determined at the IGGR, following the procedure described by Demény et al. (2016a). Sample chips of about 0.5–1 g were crushed under vacuum in stainless steel tubes, after which the released water was purified by vacuum distillation and introduced into a liquid water isotope analyzer, model LWIA-24d, produced by Los Gatos Research Ltd. It should be noted, that due to the generally large sample requirement the measured compositions represent multidecadal-centennial averages. Water contents were determined on the basis of H_2O amount extracted from inclusions and a calibration by measuring different amounts of water standards, and expressed as ppm (mg H_2O per 1000 g of calcite). Measurement drifts, amount effect, and memory effect were tested, analyzing laboratory standards (BWS-1, BWS-2, BWS-3; see Czuppon et al., 2014), along with samples, as previously described (Demény et al., 2016a; Demény et al., 2019). Prior to running samples, actual memory effect was calculated by injecting laboratory standards with very different isotopic compositions (see below). As most of the sample values were close to the BWS-2 water (see below), BWS-2 was analyzed before the extracted water samples. Once the water sample from the speleothem was analyzed and the H_2O yield was known, laboratory standards with the same amount of H_2O were measured to overcome amount effect. Finally, shifts from the theoretical compositions of the measured isotope values of water standards were used to correct the sample values. Standard deviations (1σ) of BWS-2 ($\delta^2H = -74.9$‰, $\delta^{18}O = -10.41$‰) and BWS-3 ($\delta^2H = -147.7$‰, $\delta^{18}O = -19.95$‰) laboratory standard waters (see Czuppon et al., 2018) were calculated for the corrected and selected analyses (1 μl H_2O was analyzed, first three analyses were discarded, and values were drift- and memory-corrected) for the measurement period. The standard deviations of BWS-2 δ^2H and $\delta^{18}O$ measurements were 0.6 and 0.14‰ ($n = 58$), while the BWS-3 water yielded 0.8 and 0.14‰ ($n = 60$).

The isotopic compositions of waters extracted from fluid inclusions ("flinc") are expressed as δ^2H and $\delta^{18}O_{flinc}$ values in ‰, relative to V-SMOW. The reproducibility of δ^2H and $\delta^{18}O_{flinc}$ values is ±2 and ± 0.5‰, respectively (Czuppon et al., 2014). The analytical accuracies of the speleothem inclusion-hosted water's δ^2H and $\delta^{18}O_{flinc}$

measurements are shown by the analysis of NU-2, a recently formed stalagmite (Demény et al., 2016a). The δ^2H and $\delta^{18}O_{flinc}$ values of inclusion water from the topmost 5 mm of the stalagmite (−64.8 ± 1.2‰, −9.5 ± 0.5‰, respectively) reported by Demény et al. (2016a) are very close to the values obtained in this study (−66.0‰ and 9.4‰), as well as to the drip water compositions measured at the same site (−64.7‰ and 9.4‰, Czuppon et al., 2018). Furthermore, calcite samples (HUA-8 and Sterling Mine calcites donated by Hubert Vonhof and Yuri Dublyansky) that were analyzed at independent laboratories were also measured in this study, and their isotopic compositions are plotted in Fig. 2. Sample HUA-8 was cut from a stalagmite collected in the Huagapo Cave in Peru, in the higher Andes, where precipitation waters are relatively ^2H- and ^{18}O-depleted, and the stalagmite is consequently characterized by low δ^2H and $\delta^{18}O_{flinc}$ values (−105‰ and 14‰, respectively, determined at the Vrije Universiteit Amsterdam; Hubert Vonhof, *pers. comm.*). The Sterling Mine calcite originated from Sterling Mine, Nevada, whose analyses at the University of Innsbruck yielded $\delta^2H = -107.6$‰ and $\delta^{18}O_{flinc} = -16.4$‰ (Yuri Dublyansky, *pers. comm.*). The δ^2H and $\delta^{18}O_{flinc}$ values obtained in this study are slightly more positive for the Sterling Mine calcite (by 3 and 0.5‰, respectively) and slightly more negative for the HUA-8 calcite (by 2.2 and 1.0‰, respectively) than expected, but these differences may derive from the combined effects of sample inhomogeneity and differences in laboratory protocols (de Graaf et al., 2020).

Clumped isotope analysis of carbonate samples was performed between July 2019 and June 2020 on a Thermo Scientific MAT-253 Plus isotope ratio mass spectrometer (IRMS) in the Isotope Climatology and Environmental Research Center (ICER) of the Institute for Nuclear Research (Debrecen, Hungary). Phosphoric acid digestion of the samples occurred at 70 °C in a Thermo Scientific Kiel IV automatic carbonate device, which is coupled to the IRMS by an inert, silica-coated capillary. To eliminate organic contamination from the extracted carbon dioxide gas, an additional Thermo Scientific PoraPak trap was installed between the two cold fingers of the Kiel device. The operation temperature of this trap was −30 °C. An hour-long, 120 °C cleaning and regeneration procedure of the PoraPak trap is usually required before each measurement process. After cryogenic purification, the carbon dioxide gas was measured against a working CO_2 gas (Linde AG, $\delta^{13}C_{VPDB} = -3.9$‰, $\delta^{18}O_{VPDB} = -12.5$‰, purity = 99.998%) for m/z 44–49 in micro-volume inlet mode and with the long integration dual inlet (LIDI) method (Hu et al., 2014). MAT-253 Plus IRMS has 7 Faraday cups with resistors $3 \times 10^8\Omega$, $3 \times 10^{10}\Omega$, and $1 \times 10^{11}\Omega$ for masses 44, 45, and 46, respectively, as well as $1 \times 10^{13}\Omega$ for masses 47, 47.5, 48, and 49. The carbonate clumped isotope analyses system has a similar build-up to that described in previous publications (Schmid and Bernasconi, 2010; Hu et al., 2014; Meckler et al., 2014; Müller et al., 2017; Piasecki et al., 2019).

Each carbonate sample measurement consisted of 10–12 replicate analyses of 100–120 μg aliquots, which were divided into three measurement carousels (with 46 positions) and were measured alongside carbonate standard samples with assigned values. ETH1, ETH2, and ETH3 were the standard samples (with long-term standard deviations ranging from 0.032 to 0.038‰) during Δ_{47} calculation, and IAEA-C2 was used to monitor instrument performance. The $\delta^{13}C$, $\delta^{18}O$, and Δ_{47} values of the ETH standards (Table 1 in Bernasconi et al., 2018) were used to transfer sample Δ_{47}'s results into the absolute reference frame.

The signal collection of one replicate consists of 40 cycles of a 10 s integration period. During this collection period, the initial 17–18 V intensity of m/z 47 drops down to 12–13 V. The applied working gas was measured under the same conditions. The background correction of the Isodat NT software was disabled. Peak scans at six different intensities were used to calculate the pressure baseline correction. These scans were performed before and after measurement, and the correction values were interpolated (V44-V49 ETH PBL).

Data evaluation was conducted with the Easotope application (John and Bowen, 2016), using the CO_2 clumped ETH PBL replicate analyses method and "Brand parameters" (Baertschi, 1976; Gonfiantini et al., 1995; Meijer and Li, 1998; Assonov and Brenninkmeijer, 2003; Brand et al., 2010), also called the "IUPAC" parameters (International Union of Pure and Applied Chemistry). A phosphoric acid correction factor (Δ^*_{25-70}) of 0.066 was applied (Petersen et al., 2019).

3. Results and discussion

The speleothems cover a long time period, ranging from sub-recent flowstones to a > 300 ka old flowstone that formed in different cave systems and under various climate regimes. Paleoclimatic interpretations of stable isotope compositions would be beyond the scope of this paper, thus, the isotopic compositions are not described in detail here. However, the observed relationships concerning paleotemperature calculations are discussed in the following sections. Listed in Table S2

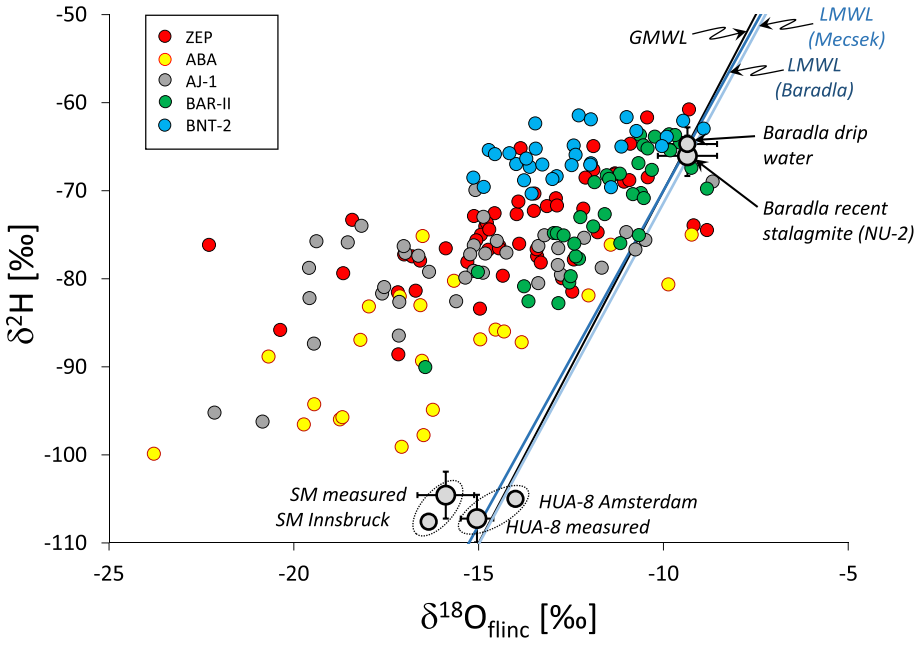

Fig. 2. Stable hydrogen and oxygen isotope compositions (in ‰ relative to V-SMOW) of inclusion-hosted waters from Hungarian speleothems (see Table S2), as well as the results of interlaboratory sample measurements. ZEP: ZEP-1 core from the Baradla cave. ABA: ABA-1 and ABA-2 cores from the Abaliget cave. AJ-1: stalagmite from the Ajándék cave. BAR-II: stalagmite from the Baradla cave. BNT-2: flowstone core from the Béke cave. See Fig. 1 for locations. SM: Sterling Mine calcite donated by Y. Dublyansky and measured at the Innsbruck University. HUA-8: calcite donated by H. Vonhof and measured at the Vrije Universiteit Amsterdam. Baradla drip water compositions are from Czuppon et al. (2018). Local meteoric water line (LMWL) for the Mecsek Mts. is $\delta^2H = 7.8 \cdot \delta^{18}O + 6.1$ (based on the 2004–2017 data of Fórizs et al., 2020), whereas for the Baradla Cave's area it is $\delta^2H = 7.5 \cdot \delta^{18}O + 6.0$ (for the period of 2013 to 2016, Czuppon et al., 2018).

are the water contents, the hydrogen and oxygen isotope compositions of inclusion waters, and the calcite oxygen isotope values averaged for the inclusion analyses samples. Clumped isotope data are listed in Table S3.

Using the stable isotope data obtained in this paper, temperature calculations may be based on i) direct $\delta^{18}O_{flinc}$ and $\delta^{18}O_{cc}$ measurements, ii) combination of measured $\delta^{18}O_{cc}$ values and $\delta^{18}O_{water}$ values calculated from $\delta^{2}H$ data, or iii) on basis of the temperature dependence of the hydrogen isotope composition of precipitation water in the region (i.e., long-term, modern-day $\delta^{2}H/T$ slopes/gradients). The procedures, advantages and drawbacks are described and discussed in the followings.

3.1. The use of $\delta^{18}O_{flinc}$ values in paleotemperature calculations

Speleothems usually form in caves from dripping water that originated as meteoric precipitation. As a result, the drip waters' hydrogen and oxygen isotope compositions generally follow global or local meteoric water lines, i.e., linear relationships in the $\delta^{2}H$-$\delta^{18}O$ plot (e.g., Rozanski et al., 1992, 1993), and inclusion-hosted water should be no exception to this relationship. However, strong shifts in the $\delta^{18}O_{flinc}$ values were previously reported (Demény et al., 2016a) and were also detected in this study (Fig. 2). Significant $\delta^{2}H$ changes from the original compositions are not assumed as the host carbonate's structure contains no hydrogen and late stage alteration that would cause hydrogen diffusion in or out is also unlikely for speleothems. The current dataset covers a large $\delta^{2}H$ range of about 40‰, and significant negative $\delta^{18}O_{flinc}$ shifts (of up to 10‰) away from the Global Meteoric Water Line (GMWL) (Fig. 2). All the researched speleothems display similar shifts, albeit to different extents. One possibility is analytical bias, i.e., methodology-related isotope fractionation that affects part of the samples. However, materials with expected isotopic compositions and samples measured at independent laboratories were also analyzed and yielded close-to-expected results. The top layers of recently formed stalagmites that cover the last few decades (NU-2 stalagmite, Demény et al., 2017b) yielded $\delta^{2}H$ and $\delta^{18}O_{flinc}$ values which were very similar to the values of the local drip water compositions (Fig. 2). The Sterling Mine calcite and the HUA-8 calcite yielded isotopic compositions along the GMWL (Fig. 2) that were similar to the expected values (see Materials and Methods section). Thus, we can conclude that the negative $\delta^{18}O_{flinc}$ shift is not related to measurement bias.

Next, we examined if secondary alteration could explain the observed negative $\delta^{18}O_{flinc}$ shift. The lower the water content of the sample, the higher the chance of late-stage oxygen isotope exchange between the water and calcite that could alter the original isotopic composition. The isotope shift was quantified by calculating the $\delta^{18}O$ value of water from the $\delta^{2}H$ values, using the GMWL equation ($\delta^{2}H = 8{\cdot}\delta^{18}O + 10$, Craig, 1961), and the difference between the calculated values and the $\delta^{18}O_{flinc}$ data were computed. The $\delta^{18}O_{flinc}$ shifts were plotted as a function of water contents, which yielded ambiguous results, with some speleothems showing positive correlations and others no correlations (Fig. S6). The ZEP-1, the AJ-1, and the BNT-2 samples had statistically significant positive correlations, while the ABA flowstone and the BAR-II stalagmite did not show significant correlations (Fig. S6). It should be noted, however, that the water content of speleothems may also depend on climate conditions (Vogel et al., 2013; Demény et al., 2013), thus, the correlations with the isotope compositions of ZEP-1, AJ-1, and BNT-2 may not necessarily indicate late-stage alteration effects. On the other hand, there is a systematic relationship between the $\delta^{2}H$ values and the $\delta^{18}O_{flinc}$ shifts for all five speleothems, which suggests that lower $\delta^{2}H$ values are associated with larger negative $\delta^{18}O_{flinc}$ shifts (Fig. S6).

Negative $\delta^{18}O_{flinc}$ shifts are difficult to explain with late-stage isotope exchange (Uemura et al., 2020), as they would require either a strong temperature decrease (that in turn would preclude diffusive isotope exchange) or an influx of a low-$\delta^{18}O$ fluid. Strong negative $\delta^{18}O_{flinc}$ shifts are related to low $\delta^{2}H$ values in glacial parts of the studied speleothems, which makes additional cooling or introduction of more ^{18}O-depleted solution unlikely. Rising cave temperatures during subsequent interglacial periods may induce re-equilibration (although, we must note that the low temperature precludes diffusion-driven exchange), in which case, the calcite-water oxygen isotope fractionation would decrease and the inclusion water would approach the host calcite composition (i.e., it would undergo a positive $\delta^{18}O_{flinc}$ shift). Mineralogical changes may induce negative $\delta^{18}O_{flinc}$ changes, if an amorphous calcium carbonate (ACC) is formed, with a small carbonate-water oxygen isotope fractionation; calcitization would result in a fractionation increase and, consequently, a negative $\delta^{18}O_{flinc}$ shift (Demény et al., 2016a, 2016b). The ACC is inferred to have a $\delta^{18}O$ value that is at least 2.4‰ lower than that of calcite precipitating at the same conditions (Demény et al., 2016b). However, this fractionation would not explain the observed ~10‰ shift.

Another explanation may be the preferential and non-equilibrium bonding of ^{18}O to the calcite structure, causing the inclusion water to be ^{18}O-depleted. The lower the formation temperature, the higher the degree of ^{18}O-bonding, whereas the opposite means that rising temperature results in approaching a thermodynamic equilibrium, analogous to the clumping of rare heavy isotopes in the carbonate structure (Eiler, 2007). Extraction of ^{18}O from the water would not appear in the calcite composition, due to the large mass difference between the two compounds. However, in the absence of evidence, the explanation of preferential removal of ^{18}O from the trapped inclusion water is speculative and requires further research. Whatever process caused the observed $\delta^{18}O_{flinc}$ shift, the data are not appropriate for temperature calculation. This observation is demonstrated by the large and unrealistic temperature values (from −39 to 22 °C, with an average of −7 °C, Fig. 3A, Supplementary Table S2).

3.2. Combined application of $\delta^{18}O_{cc}$ and $\delta^{2}H_{flinc}$ values in paleotemperature calculations

In this paleotemperature calculation approach, the oxygen isotope composition of water is calculated from the $\delta^{2}H$ value and from the actual global or local meteoric water line (GMWL or LMWL), and the fractionation between the calculated water value and the measured calcite $\delta^{18}O_{cc}$ may provide the absolute temperature, if the fractionation-temperature relationship is known (Zhang et al., 2008). The uncertainties in fractionation equations have been widely discussed (e.g., Daëron et al., 2019). As a compromise, an intermediate equation (Eq. 1) between those of Coplen (2007) and Tremaine et al. (2011) (in the ratio of 65% and 35%, respectively) was selected for the present study, as this relationship was found for the local settings (Demény et al., 2016b).

$$1000{\cdot}\ln\alpha(\text{calcite}-\text{H}_2\text{O}) = 0.65{\cdot}(17,400/\text{T}–28.6) + 0.35{\cdot}(16,100/\text{T}–24.6) \quad (1)$$

Additionally, the hydrogen and oxygen isotope data must be corrected for changes in the oceanic source composition, which is related to ice volume variation throughout glacial-interglacial cycles. The correction procedure is based on the method of Spratt and Lisiecki (2016), who suggested corrections using the relationship between sea level and the $\delta^{18}O$ values of ocean water. The $\delta^{2}H$ correction was obtained by multiplying the $\delta^{18}O$ correction by 8 (based on the GMWL equation in Craig, 1961). A temperature error of 1.6 °C was obtained by assuming ±0.1‰ and ± 2‰ measurement uncertainties for $\delta^{18}O_{cc}$ and $\delta^{2}H$, respectively, and calculating with worst-case scenario (both uncertainties acting in the same direction). This calculation yielded a paleotemperature record (Supplementary Table S2) with large fluctuations (Fig. 3B, open circles) that are unrealistic within the local environmental parameters. Speleothem formation temperatures below 0 °C are impossible, because there would not be a drip water supply at those

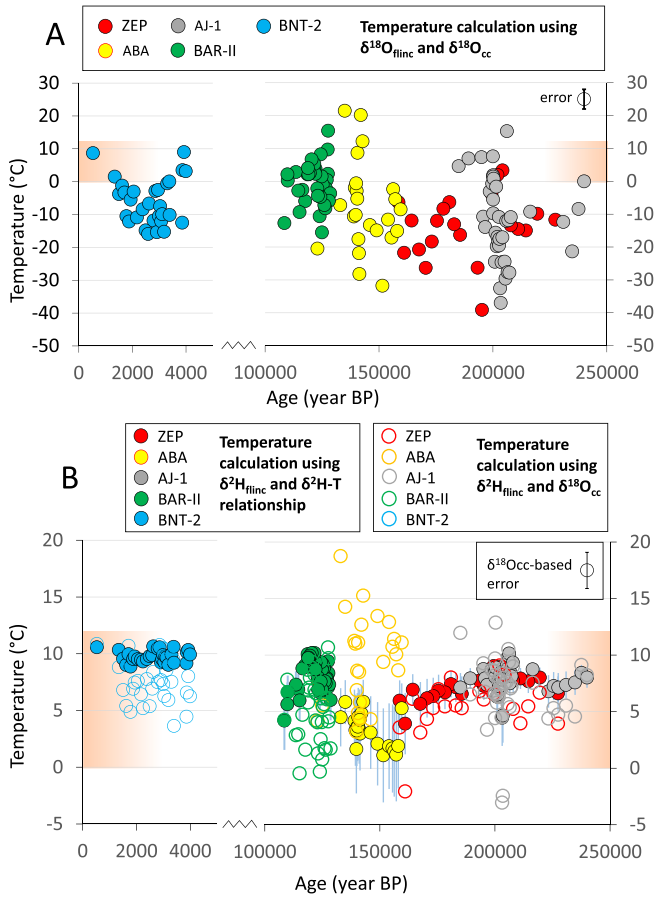

Fig. 3. A). Paleotemperature data yielded by the combined application of stable oxygen isotope compositions of calcite ($\delta^{18}O_{cc}$) and fluid inclusion water ($\delta^{18}O_{flinc}$). B) Paleotemperature data obtained from hydrogen isotope analyses of inclusion waters (δ^{2}H-based) and from the combined use of δ^{2}H values and oxygen isotope analysis of speleothem calcite ($\delta^{18}O_{cc}$-based). Shaded areas mark the range of realistic temperatures that can be inferred from the studied speleothems (see text). Temperature errors were calculated using error propagation of analytical and δ^{2}H/T gradient uncertainties (see text). Calculated errors are smaller than the dot size for the BNT-2 samples. The $\delta^{18}O_{cc}$-based temperatures have a uniform uncertainty of ±1.6 °C originated from analytical precisions.

temperatures. Temperatures reaching 19 °C at the last interglacial (at about 120 ka BP, Fig. 3) are also unrealistic, even during the interglacial periods, as temperatures would have needed to be about 9 °C warmer than in the present day. On the contrary, the last interglacial was approximately 1.5 °C warmer on a global scale than the present day (Turney and Jones, 2010). Furthermore, a maximum temperature anomaly of +4.3 °C relative to the present day was found at a high-altitude cave in the Italian Alps by Johnston et al. (2018). Thus, Fig. 3 shows a realistic temperature range of 0 to 12 °C as a reference.

3.3. The use of $\delta^{2}H$ values in paleotemperature calculations

The third approach is based on the temperature dependence of the hydrogen isotope composition of precipitation water in the region (i.e., long-term, modern-day δ^{2}H/T slopes/gradients). Affolter et al. (2019) used an equivalent approach and a recent δ^{2}H/T gradient for a 14-ka long record from the Milandre cave (Switzerland) that included the Younger Dryas and the Holocene, as well. The local composition-temperature relationship for the Baradla Cave's area was studied in previous research (Demény et al., 2017a), via monitoring over several years. However, as Kern et al. (2019) elucidated, longer-term monitoring provides more robust and coherent relationships in the wider region. The empirical δ^{2}H/T slope was determined for modern precipitation (1980–2018) surrounding the study area (Fig. 1). Monthly precipitation stable hydrogen isotope compositions were extracted from the Global Network of Isotopes in Precipitation (GNIP; http://www.isohis.iaea.org) database for the five nearest GNIP stations with more than 10 years of data between 1980 and 2018: Krakow (Poland), Liptovsky Mikulas (Slovakia), Vienna (Austria), Ljubljana (Slovenia), and Zagreb (Croatia). The monthly records were updated with recently published data for Ljubljana (Kern et al., 2020a) and Zagreb (Krajcar Bronić et al., 2020). Monthly gridded (0.25 deg. x 0.25 deg., approx 30 km) precipitation-amount and surface air temperature data were retrieved (*E*-OBS 21.0e, Cornes et al., 2018) from the grid cell nearest to the GNIP stations to infer annual mean and winter half-year (October to March) δ^{2}H-temperature gradients. As a criterion for incomplete years, amount-weighted annual and winter half-year mean δ^{2}H values were only computed if the δ^{2}H data represented more than 85% of the precipitation total of the considered time interval (annual or winter), as it was the critical threshold for precipitation tritium (Kern et al., 2020b).

Linear regression slopes were calculated between the amount-weighted annual/winter δ^{2}H and the corresponding seasonal mean temperature to determine the site-specific modern day δ^{2}H/T (‰ °C^{-1}) gradient. The analysis returned a significant ($p < 0.1$) positive slope for each station, and the gradient varied between 3.64 and 6.45‰ °C^{-1} for winter, and 2.27 and 5.38‰ °C^{-1} for the annual mean (Fig. 1, Table S4). Finally, the inverse distance weighted mean δ^{2}H/T slopes were calculated for each cave location, using distances from the GNIP stations (Fig. 1, Table S4). This procedure yielded δ^{2}H/T gradient values of 5.0‰ °C^{-1} for the Baradla and the Ajándék caves, and 4.7‰ °C^{-1} for the Abaliget cave, which values are very close to the δ^{2}H/T gradient of 4.8‰ °C^{-1} inferred from the average mid-latitude δ^{18}O/T gradient of 0.6‰ °C^{-1} (Rozanski et al., 1992). The value of 5.0‰ °C^{-1} was applied for the ZEP-1, BAR-II, BNT-2, and AJ-1 samples, while the 4.7‰ °C^{-1} value was used for the ABA-1 and ABA-2 samples. Demény et al. (2017a) and (Demény et al., 2019) used lower δ^{2}H/T gradient values (about 2 to 3.5‰ °C^{-1}), based on local precipitation monitoring spanning about two years. The large (up to >10 °C) variations in the calculated temperatures of Demény et al. (2017a) and (Demény et al., 2019) may derive from the use of δ^{2}H/T gradient values that are too low and should therefore be revised in later studies.

For paleotemperature calculations, winter half-year precipitation δ^{2}H/T gradients were used, as local cave drip waters derive predominantly from cold season infiltration (Czuppon et al., 2018). One of the primary issues of using modern δ^{2}H/T gradient values is that the isotope-temperature relationship may change with time. The δ^{18}O/T gradient calculated for non-overlapping, multiannual periods using long-term precipitation isotope data from Zagreb was slightly different but nevertheless statistically indistinguishable (Krajcar Bronić et al., 2020), suggesting that the empirical δ^{18}O/T relationship at a given location is robust at the sub-centennial time scale. Although the local δ^{2}H/T variations at the researched caves are unknown, previous studies on meteoric water and groundwater in the Great Hungarian Plain (East Hungary) indicate subtle changes from recent to glacial times. A δ^{18}O/T gradient of 0.32‰ °C^{-1} was found during a 9-year long precipitation monitoring sequence in Debrecen (East Hungary, Vodila et al., 2011), whereas a slightly higher δ^{18}O/T value of 0.38‰ °C^{-1} was calculated using differences in δ^{18}O values and noble gas temperatures of Holocene and pre-Holocene (>20 ka BP) groundwaters (Varsányi et al., 2011). The 0.06‰ °C^{-1} difference between the recent and fossil values would correspond to an approximately 0.5‰ °C^{-1} δ^{2}H/T increase, if the glacial period is included. These small changes suggest that the empirical δ^{18}O/T relationship at a given location is robust even at glacial-interglacial time scales. However, the uncertainties of winter half-year gradients (expressed as standard error, SE) are rather high (1.7 to 2.7 SE) compared to the annual gradients (0.8 to 1.6 SE, Table S4). The propagated standard errors for the cave location gradients are 2.1 to 2.3 for

the winter half-year and 1.2 to 1.3 for the annual data. Based on these considerations and due to the use of the winter gradient values in the temperature calculations, a tentative 2.2‰ °C^{-1} uncertainty is used for the propagated error calculations, which represents a maximum error estimation.

The shifts of source-corrected δ^2H values (see above) from the modern-day values were calculated and divided by the δ^2H/T gradients to obtain the shift from the modern-day temperature. This procedure yields long-term surface temperatures (Table S2). The δ^2H-derived temperatures in Fig. 3B show a realistic temperature range. The minimum temperature yielded for the ~150 ka old glacial period is 1.1 ± 4 °C, while the maximum temperature is 10.7 ± 0.3 °C in the Holocene, 10.2 ± 0.1 °C in the last interglacial (MIS5, about 120 ka ago), and 10.1 ± 0.1 °C in the MIS7 interglacial, approximately 200 ka ago. Uncertainties of the δ^2H-derived temperatures were calculated using error propagation with the following conditions: δ^2H and δ^2H/T gradient uncertainties are ±2‰ and ± 2.2‰ °C^{-1}, respectively, and the uncertainties follow the Gaussian probability distribution. The average propagated error for the entire dataset is 1.1 °C. We have to emphasize, however, that the error propagation calculation is based on the assumption that the uncertainties follow Gaussian probability distribution, which may not be valid for the isotope data and for the δ^2H/T gradient estimation. The ±2‰ uncertainty in the δ^2H values may itself induce a temperature uncertainty of 0.5 °C, which can be considered as the lowest limit of temperature error. Another source of uncertainty derives from the estimation of the δ^2H/T relationship, as there is no information about the δ^2H/T variation on the multimillennial age scale. However, the winter-based 2.2‰ °C^{-1} uncertainty is thought to be a maximum value, as the annual values (based on larger datasets) have much lower scatter, and the glacial-interglacial change are associated with much smaller δ^2H/T variation (see above). The interglacial periods (0–11 ka BP, 115–130 ka BP, 200–215 ka BP) yielded an average temperature error of ±0.6 °C, while glacial periods (108–115 ka BP, 130–200 ka BP, 215–227 ka BP in the present dataset) yielded an average temperature error of ±2.4 °C due to the large (up to 40‰) δ^2H shift from the present day drip water compositions.

To test if the δ^2H-derived temperatures are reliable, clumped isotope analyses were performed on the ZEP-1 flowstone core, because it covers several glacial-interglacial periods (and thus large temperature ranges). Additionally, unlike stalagmites, cave-hosted flowstones appear to yield close-to-equilibrium Δ_{47} values (e.g., the Havasok cave tufa deposit that was studied by Kele et al., 2015 and can be classified as a flowstone, being a sheet-like, cave-hosted carbonate deposit formed on rock surface). Also unlike stalagmites, whose carbonate is precipitated from dripping water due to fast CO_2 degassing, flowstones are formed from a water film flowing down on a rock surface. Thus, they are transitional between stalagmites and subaqueous carbonate formations, the latter yielding close-to-equilibrium clumped isotope values (Daëron et al., 2019).

The topmost part (upper 2 mm) and a sample at 10 mm from the top of the BNT-2 flowstone were measured for comparison. Based on the age data of Demény et al. (2019), the topmost sample covered the last decades based on radiocarbon activity measurements, whereas the sample at 10 mm had an age of about 520 yr BP (Before Present). The Δ_{47} data (see Table S3) were plotted as a function of δ^2H-derived temperatures (for the ZEP-1 samples and for the BNT-2/10 mm sample) and monitored cave air temperature (for the topmost BNT-2 sample) in Fig. 4. The ZEP-1 and the BNT-2 flowstone data scatter around the Jautzy et al. (2020) equilibrium line, which indicates that the δ^2H-derived temperatures are realistic. Further evaluation of the clumped isotope data requires the inspection of kinetic and equilibrium isotope fractionations, as discussed in the following section.

3.4. Calcite-water oxygen isotope fractionations

As discussed, paleotemperature reconstructions using calcite oxygen isotope compositions appear to be unreliable, yielding unrealistically high and low temperatures. Secondary, post-formational diagenetic processes can be excluded as a major cause, because cave environments are isolated, stable in the geological time scale, and usually untouched by exotic fluids that could change the isotopic compositions of the carbonates. In contrast, primary processes related to formation, such as kinetic fractionations and changes in the physiochemical conditions, can significantly influence the δ^{18}O value of the precipitated calcite, with both scenarios affecting the calcite-water oxygen isotope fractionation (Dietzel et al., 2009; Watkins et al., 2014). Once the $\delta^{18}O_{cc}$ value is

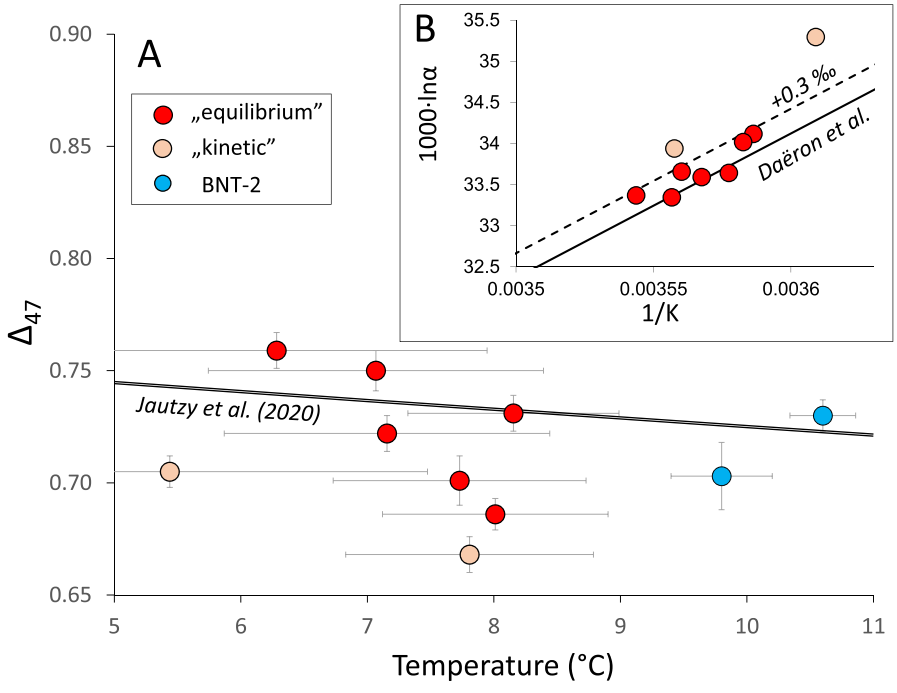

Fig. 4. A) Clumped isotope compositions (Δ_{47}) of the ZEP-1 and BNT-2 flowstones as a function of temperature. Temperatures are δ^2H-based for the ZEP-1 samples and monitoring-based for the BNT-2 samples. Red dots: ZEP-1 samples with no detected kinetic shift in δ^{18}O values. Pink dots: ZEP-1 samples with detected kinetic shift in δ^{18}O values. Blue dots: BNT-2 samples. Solid line: Jautzy et al. (2020). Uncertainties: standard error for Δ_{47} data and error-propagated standard deviation for the temperature data. B) 1000·lnα(calcite-water) values vs. 1/K for samples measured for clumped isotope compositon. Solid line: Daëron et al. (2019); dashed line: the Daëron et al. (2019) curve +0.3‰. See text for details. (For interpretation of the references to colour in this figure legend, the reader is referred to the web version of this article.)

measured and source-corrected (see above), and the $\delta^{18}O_{water}$ value is calculated from the source-corrected hydrogen isotope compositions, the calcite-water oxygen isotope fractionation is obtained and expressed by 1000·lnα, where $\alpha = (^{18}O/^{16}O_{cc})/(^{18}O/^{16}O_{water})$. The 1000·lnα values can be plotted as a function of δ^2H-derived formation temperature to understand the impact of kinetic effects and physiochemical changes. The calculated 1000·lnα values and the δ^2H-derived temperatures would be automatically correlated, if the $\delta^{18}O_{cc}$ data were constant, with a slope of 0.63 °C^{-1}. The ~25‰ δ^2H change observed for the individual speleothems (Fig. 2) would correspond to a $\delta^{18}O_{water}$ change of approximately 3‰, which is transferred to the $\delta^{18}O_{cc}$ data through the calcite-water oxygen isotope fractionation. Changing the $\delta^{18}O_{cc}$ values would decrease the slope of the linear 1000·lnα–temperature correlation to reach an equilibrium calcite-water isotope fractionation. Deviations from the equilibrial calcite-water 1000·lnα–temperature relationships may indicate kinetic fractionation or changes in physiochemical conditions. Fig. 5 shows that the oxygen isotope compositions of the calcites change, along with the δ^2H-derived $\delta^{18}O_{water}$ values, by about 7‰, that makes the automatic 1000·lnα–temperature correlation unlikely.

Fig. 6. shows calculated 1000·lnα values as a function of temperature with a large spread, as well as with systematic distributions. Most of the speleothems yielded positive 1000·lnα–1/T relationships, starting from "equilibrium" values around the fractionation curve of Daëron et al. (2019) and trending toward higher 1000·lnα values at lower temperatures. This shift can be explained by the increasingly dry conditions during cooling (see Demény et al., 2017a for the Baradla Cave cases). A reduction in the precipitation amount increases the chance of degassing, evaporation, and Prior Calcite Precipitation along the karstic water seepage route, leading to kinetic isotope fractionation and ^{18}O-enrichment in the precipitated calcite (Riechelmann et al., 2013).

In contrast, the shifts to low 1000·lnα with decreasing temperature can be attributed to changes in the solution chemistry. The equation of Kim and O'Neil (1997) was obtained in calcite-precipitating experiments, applying higher pH values in the solution than are present in modern-day conditions in the studied caves (Czuppon et al., 2018). Studies on calcite-water oxygen isotope fractionation showed decreasing 1000·lnα values with increasing pH (Watkins et al., 2014; Kluge et al., 2018). Glacial conditions, which are presumed for the ABA flowstone (Koltai et al., 2017), produce low temperatures and reduced soil CO_2 production, leading to higher pH in the infiltrating solution. This process may explain the negative shift observed in the 1000·lnα values obtained for the ABA flowstone (Fig. 6) toward the Kim and O'Neil (1997) curve.

However, some of the ABA data are shifted toward even lower 1000·lnα values. An additional explanation can be found in mineralogical changes, i.e., in the extensive formation of ACC with low ACC-water oxygen isotope fractionation (Demény et al., 2016b), which is preserved in the recrystallized calcite (Demény et al., 2016a).

The observed positive 1000·lnα-1/T trends (Fig. 6) have another implication. The Daëron et al. (2019) curve is based on data from extremely slowly growing carbonate (including the Devils Hole calcite reported by Coplen, 2007) and therefore can be interpreted to be the closest to equilibrium. Samples shifted from this equilibrium toward higher 1000·lnα values that exceed the analytical uncertainties (~0.3‰, Fig. 4B) may be regarded as kinetically influenced, and their data can be excluded from the interpretations. The ZEP-1 data scatter on the Δ_{47}-temperature plot (Fig. 4) is slightly reduced, when the kinetically affected samples (pink dots in Fig. 4) are excluded. The "equilibrium" samples are plotted close to the Daëron et al. (2019) curve indicating that not only are the δ^2H-derived temperatures realistic, but also that the calculated 1000·lnα-temperature relationship can be used to filter the samples to obtain more reliable clumped isotope data for cave-hosted flowstones.

4. Conclusions

Speleothems spanning the last ~250 ka and various formation environments (stalagmite or flowstone) were collected from several caves in Hungary, and the stable isotope compositions of calcites and inclusion-hosted waters were determined for 156 samples. The data were used in paleotemperature calculations based on three approaches.

i) Direct determination of calcite-water oxygen isotope fractionation by measuring the $\delta^{18}O$ values of calcite and inclusion water.

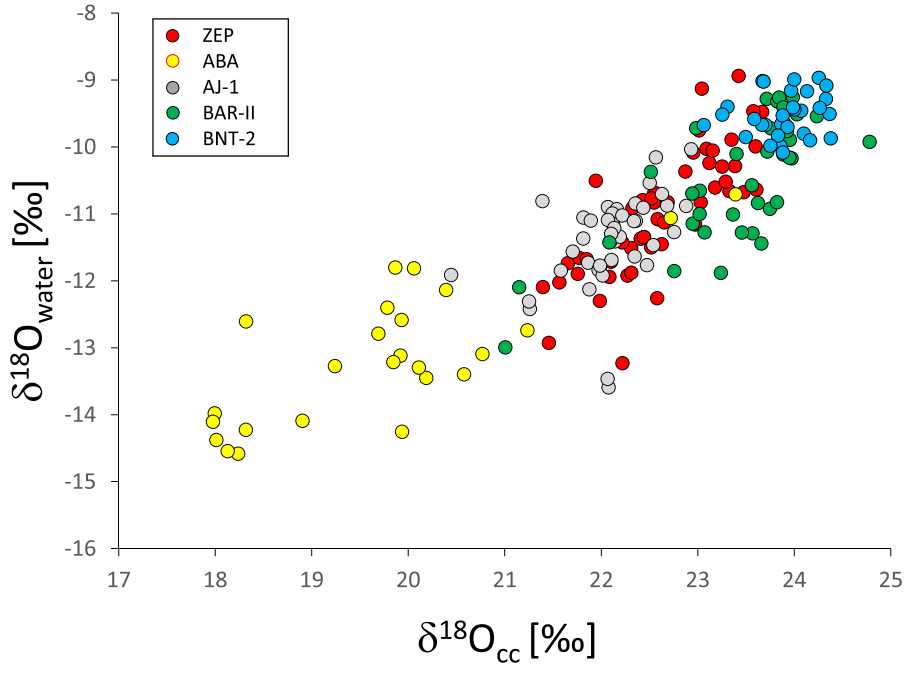

Fig. 5. Calculated $\delta^{18}O_{water}$ values (see text for calculation procedure) as a function of calcite $\delta^{18}O_{cc}$ data (both in ‰ relative to V-SMOW). Speleothems are marked as in Fig. 2. Linear regression calculation for the entire dataset yield an R^2 value of 0.8.

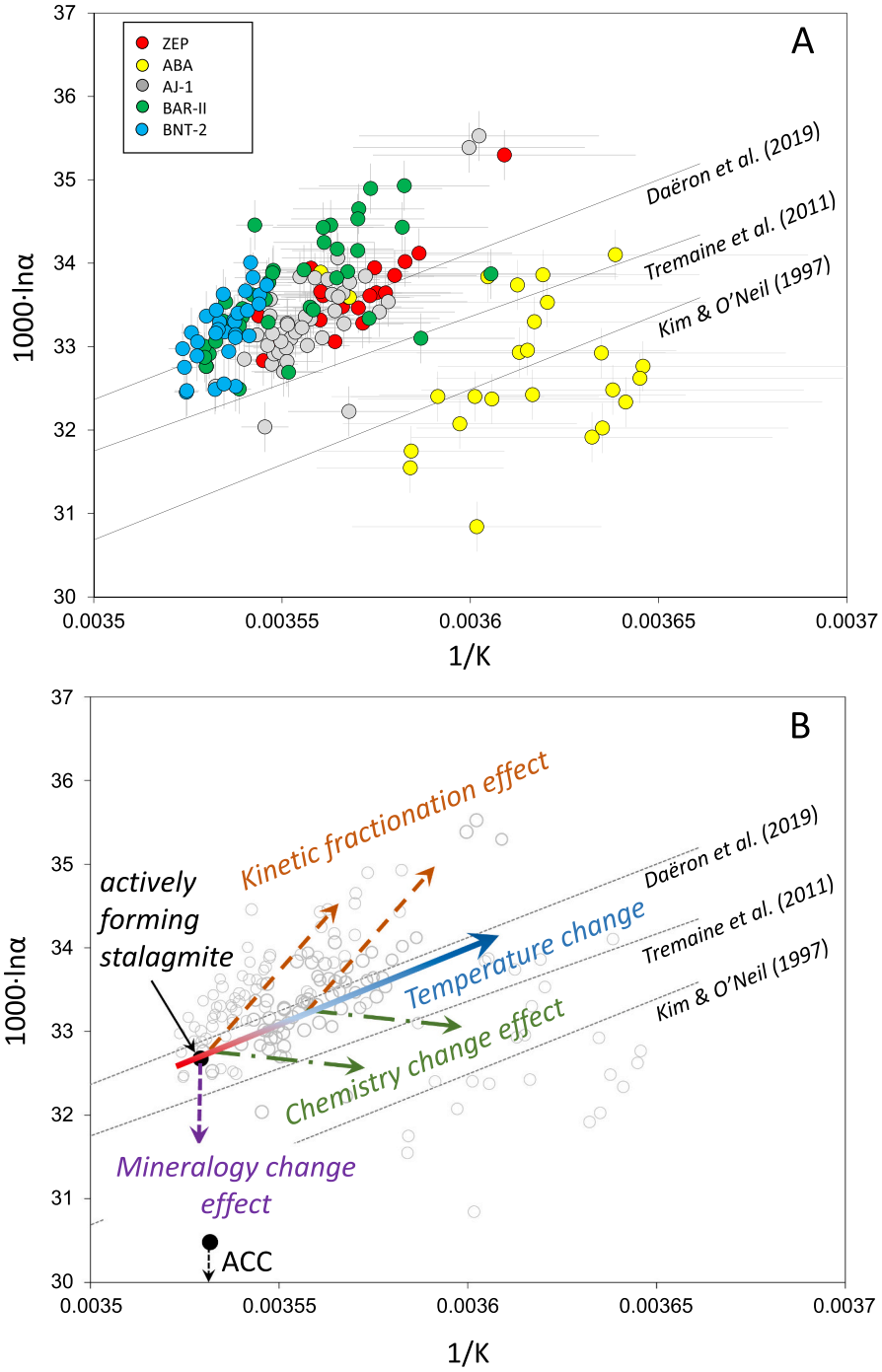

Fig. 6. A) Calcite-water oxygen isotope fractionation values as a function of δ^2H-based temperatures (in 1/K) for speleothems (marked as in Fig. 2). The uncertainties related to analytical precision and temperature calculations are indicated only for the ABA flowstone data to clarify the fig. B) Main processes affecting the calcite-water oxygen isotope fractionation value. ACC: amorphous calcium carbonate (the arrow indicates that the fractionation value is a lower estimation, see Demény et al., 2016b).

The δ^{18}O values of inclusion waters determined for Hungarian speleothems show an increasingly negative shift from the Global Meteoric Water Line, with decreasing δ^2H values, which may be due to the combined effects of diagenetic alteration, mineralogical changes, and preferential bonding of ^{18}O to the calcite structure. The strong δ^{18}O shift precludes the use of direct calcite-water oxygen isotope measurement in paleotemperature calculation.

ii) Calculation of water δ^{18}O values from the hydrogen isotope composition of inclusion-hosted water and global or local meteoric water lines, direct measurement of calcite composition, and temperature calculation, using known fractionation-temperature relationships. The unrealistic temperatures yielded by this approach indicate that the calcite δ^{18}O values may have been affected by *syn*- and post-formational processes, such as kinetic fractionation and late-stage isotope exchange. More data on diagenetically altered speleothem formations and additional experimental studies are needed to decipher the background processes.

iii) Calculation of ambient temperature from the hydrogen isotope composition of inclusion-hosted water. This calculation requires the local long-term composition-temperature relationship for precipitation waters, the modern-day temperature, and the drip water composition. The precision of the calculations depends on the δ^2H difference between recent drip water composition and the actual period's δ^2H value (1‰ increase corresponds to

~0.2 °C calculated temperature rise), as well as on the knowledge of the δ^2H/T gradient (1‰ °C^{-1} increase causes ~0.4 °C higher calculated temperature). The composition-temperature relationships were determined for the study area by collecting amount-weighted annual and winter half-year mean δ^2H values from the Global Network of Isotopes in Precipitation and monthly-gridded surface temperatures. Clumped isotope analyses of a flowstone layer supported the inferred δ^2H-based temperatures. The calculations yielded paleotemperature data for the last ~250 ka ranging from 1.1 ± 4 °C (MIS6 glacial period) to 10.7 ± 0.3 °C (Holocene). Future studies on potential changes in the δ^2H/T gradient are needed to determine the degree of temporal δ^2H/T variations and their effects on the paleotemperature calculations.

Declaration of Competing Interest

The authors have no competing interests to declare.

Acknowledgements

The study was supported financially by the National Research, Development and Innovation Office, Hungary (OTKA 101664 and PD 121387) and the Hungarian Academy of Sciences (NANOMIN project, KEP-8/2018, ELKH KEP-1/2020). The clumped isotope facility of the Institute for Nuclear Research was supported by the European Union and the State of Hungary, co-financed by the European Regional Development Fund in the project of GINOP-2.3.2-15-2016-00009 'ICER'. U—Th dating was funded by the Science Vanguard Research Program of the Ministry of Science and Technology (MOST) (109-2123-M-002-001 to C.-C. S.), the National Taiwan University (109L8926 to C.-C.S.), and the Higher Education Sprout Project of the Ministry of Education, Taiwan ROC (108L901001 to C.-C.S.). We are grateful to Drs. Yuri Dublyansky and Hubert Vonhof for their generous donations of intercomparison materials. We also acknowledge the *E*-OBS dataset from the EU-FP6 project UERRA (http://www.uerra.eu) and thank the data providers in the ECA&D project (https://www.ecad.eu). Permissions for speleothem sampling were provided by the Duna-Ipoly and the Aggtelek National Parks. We thank Michael Böttcher for flexible editorial handling and three anonymous reviewers for their critical remarks and suggestions that helped improve the paper. Ariana Gugora is gratefully thanked for careful proofreading.

Appendix A. Supplementary data

Supplementary data to this article can be found online at https://doi.org/10.1016/j.chemgeo.2020.120051.

References

Yonge, C.J., 1982. Stable Isotope Studies of Water Extracted from Speleothems. PhD thesis. McMaster University, Hamilton, ON, Canada (pp. 270).
Affolter, S., Fleitmann, D., Leuenberger, M., 2014. New online method for water isotope analysis of speleothem fluid inclusions using laser absorption spectroscopy (WS-CRDS). Clim. Past 10, 1291–1304.
Affolter, S., Häuselmann, A., Fleitmann, D., Edwards, R.L., Cheng, H., Leuenberger, M., 2019. Central Europe temperature constrained by speleothem fluid inclusion water isotopes over the past 14,000 years. Sci. Adv. 5, eaav3809.
Allan, M., Fagel, N., van der Lubbe, H.J.L., Vonhof, H.B., Cheng, H., Edwards, R.L., Verheyden, S., 2018. High-resolution reconstruction of 8.2-ka BP event documented in Père Noël cave, southern Belgium. J. Quat. Sci. 33, 840–852.
Arienzo, M.M., Swart, P.K., Vonhof, H.B., 2013. Measurement of δ^{18}O and δ^2H values of fluid inclusion water in speleothems using cavity ring-down spectroscopy compared with isotope ratio mass spectrometry. Rapid Commun. Mass Spectrom. 27, 2616–2624.
Assonov, S.S., Brenninkmeijer, C.A.M., 2003. A redetermination of absolute values for $^{17}R_{VPDB\text{-}CO2}$ and $^{17}R_{VSMOW}$. Rapid Com. Mass. Spec. 17, 1017–1029.
Baertschi, P., 1976. Absolute ^{18}O content of standard mean ocean water. Earth Planet. Sci. Lett. 31, 341–344.
Bernasconi, S.M., Müller, I.A., Bergmann, K.D., Breitenbach, S.F.M., Fernandez, A., Hodell, D.A., Jaggi, M., Meckler, A.N., Millan, I., Ziegler, M., 2018. Reducing uncertainties in carbonate clumped isotope analysis through consistent carbonate-based standardization. Geochem. Geophys. Geosyst. 19, 2895–2914.
Brand, W.A., Assonov, S.S., Coplen, T.B., 2010. Correction for the ^{17}O interference in $\delta(^{13}C)$ measurements when analyzing CO_2 with stable isotope mass spectrometry (IUPAC Technical Report). Pure Appl. Chem. 82, 1719–1733.
Coplen, T.B., 2007. Calibration of the calcite-water oxygen-isotope geothermometer at Devils Hole, Nevada, a natural laboratory. Geochim. Cosmochim. Acta 71, 3948–3957.
Cornes, R.C., van der Schrier, G., van den Besselaar, E.J.M., Jones, P.D., 2018. An Ensemble Version of the E-OBS Temperature and Precipitation Data Sets. J. Geophys. Res. Atmos. 123, 9391–9409.
Craig, H., 1961. Isotopic variations in meteoric waters. Science 133, 1702–1703.
Czuppon, Gy, Ramsay, R.R., Özgenc, I., Demén, Y.A., Gwalani, L.G., Rogers, K., Eves, A., Papp, L., Palcsu, L., Berkesi, M., Downes, P.J., 2014. Stable (H, O, C) and noble-gas (He and Ar) isotopic compositions from calcite and fluorite in the Speewah Dome, Kimberley Region, Western Australia: implications for the conditions of crystallization and evidence for the influence of crustal-mantle fluid mixing. Mineral. Petrol. 108, 759–775.
Czuppon, Gy, Demény, A., Leél-Őssy, Sz, Óvari, M., Molnár, M., Stieber, J., Kiss, K., Kármán, K., Surányi, G., Haszpra, L., 2018. Cave monitoring in the Béke and Baradla caves (Northeastern Hungary): implications for the conditions for the formation cave carbonates. Int. J. Speleol. 47, 13–28.
Daëron, M., Drysdale, R.N., Peral, M., Huyghe, D., Blamart, D., Coplen, T.B., Lartaud, F., Zanchetta, G., 2019. Most Earth-surface calcites precipitate out of isotopic equilibrium. Nat. Commun. 10, 429.
Demény, A., Czuppon, Gy, Siklósy, Z., Leél-Őssy, Sz, Lin, K., Shen, Ch., Gulyás, K., 2013. Mid-Holocene climate conditions and moisture source variations based on stable H, C and O isotope compositions of speleothems in Hungary. Quat. Int. 293, 150–156.
Demény, A., Czuppon, Gy, Kern, Z., Leél-Őssy, Sz, Németh, A., Szabó, M., Tóth, M., Wu, Ch-Ch., Shen, Ch., Molnár, M., Németh, T., Németh, P., Óvári, M., 2016a. Recrystallization-induced oxygen isotope changes in inclusion-hosted water of speleothems – Paleoclimatological implications. Quat. Int. 415, 25–32.
Demény, A., Németh, P., Czuppon, Gy, Leél-Őssy, Sz, Szabó, M., Judik, K., Németh, T., Stieber, J., 2016b. Formation of amorphous calcium carbonate in caves and its implications for speleothem research. Sci. Rep. 6, 39602.
Demény, A., Kern, Z., Czuppon, Gy, Németh, A., Leél-Őssy, Sz, Siklósy, Z., Lin, K., Hsun-Ming, H., Shen, Ch-Ch., Vennemann, T.W., Haszpra, L., 2017a. Stable isotope compositions of speleothems from the last interglacial – Spatial patterns of climate fluctuations in Europe. Quat. Sci. Rev. 161, 68–80.
Demény, A., Németh, A., Kern, Z., Czuppon, Gy, Molnár, M., Leél-Őssy, Sz, Óvári, M., Stieber, J., 2017b. Recently forming stalagmites from the Baradla Cave and their suitability assessment for climate-proxy relationships. Central Eur. Geol. 60, 1–34.
Demény, A., Kern, Z., Németh, A., Frisia, S., Hatvani, I.G., Czuppon, Gy, Leél-Őssy, Sz, Molnár, M., Óvári, M., Surányi, G., Gilli, A., Wu, Ch.-Ch., Shen, Ch.-Ch., 2019. North Atlantic influences on climate conditions in East-Central Europe in the late Holocene reflected by flowstone compositions. Quat. Int. 512, 99–112.
Dietzel, M., Tang, J., Leis, A., Köhler, S.J., 2009. Oxygen isotopic fractionation during inorganic calcite precipitation — Effects of temperature, precipitation rate and pH. Chem. Geol. 268, 107–115.
Eiler, J.M., 2007. "Clumped-isotope" geochemistry—the study of naturally-occurring, multiply-substituted isotopologues. Earth Planet. Sci. Lett. 262, 309–327.
Fórizs, I., Kern, Z., Csicsák, J., Csurgó, G., Földing, G., Máthé, Z., Ország, J., Szreda, G., Vendégh, R., 2020. Monthly data of stable isotopic composition (δ^{18}O, δ^2H) and tritium activity in precipitation from 2004 to 2017 in the Mecsek Hills, Hungary. Data Brief 32, 106206.
Gonfiantini, R., Stichler, W., Rozanski, K., 1995. Standards and intercomparison materials distributed by the International Atomic Energy Agency for stable isotope measurements. In: Reference and Intercomparison Materials for Stable Isotopes of Light Elements, IAEA-TECDOC-825. International Atomic Energy Agency, Vienna, pp. 13–29.
de Graaf, S., Vonhof, H.B., Weissbach, T., Wassenburg, J.A., Levy, E.J., Kluge, T., Haug, G.H., 2020. A comparison of isotope ratio mass spectrometry and cavity ring-down spectroscopy techniques for isotope analysis of fluid inclusion water. Rapid Commun. Mass Spectrom. 34, e8837.
Harmon, R.S., Schwarcz, H.P., 1981. Changes in ^{2}H and ^{18}O enrichment of meteoric water and Pleistocene glaciations. Nature 290, 125–128.
Hodell, D.A., Turchyn, A.V., Wiseman, C.J., Escobar, J., Curtis, J.H., Brenner, M., Gilli, A., Mueller, A.D., Anselmetti, F., Ariztegui, D., Brown, E.T., 2012. Late Glacial temperature and precipitation changes in the lowland Neotropics by tandem measurement of δ^{18}O in biogenic carbonate and gypsum hydration water. Geochim. Cosmochim. Acta 77, 352–368.
Hu, B., Radke, J., Schlüter, H.-J., Heine, F.T., Zhou, L., Bernasconi, S.M., 2014. A modified procedure for gas-source isotope ratio mass spectrometry: the long-integration dual-inlet (LIDI) methodology and implications for clumped isotope measurements. Rapid Commun. Mass Spectrom. 28, 1413–1425.
Jautzy, J.J., Savard, M.M., Dhillon, R.S., Bernasconi, S.M., Smirnoff, A., 2020. Clumped isotope temperature calibration for calcite: Bridging theory and experimentation. Geochem. Persp. Let. 14, 36–41.
John, C.M., Bowen, D., 2016. Community software for challenging isotope analysis: first applications of 'Easotope' to clumped isotopes. Geochem. Geophys. Geosyst. 30, 2285–2300.
Johnston, V.E., Borsato, A., Frisia, S., Spötl, C., Dublyansky, Y., Töchterle, P., Hellstrom, J.C., Bajo, P., Edwards, R.L., Cheng, H., 2018. Evidence of thermophilisation and elevation-dependent warming during the last Interglacial in the Italian Alps. Sci. Rep. 8, 2680.

Kele, S., Breitenbach, S.F.M., Capezzuoli, E., Meckler, N., Ziegler, M., Millan, I.M., Kluge, T., Deák, J., Hanselmann, K., John, C.M., Yan, H., Liu, Z., Bernasconi, S.M., 2015. Temperature dependence of oxygen- and clumped isotope fractionation in carbonates: a study of travertines and tufas in the 6–95 °C temperature range. Geochim. Cosmochim. Acta 168, 172–192.

Kern, Z., Demény, A., Persoiu, A., Hatvani, I.G., 2019. Speleothem Records from the Eastern part of Europe and Turkey – Discussion on Stable Oxygen and Carbon Isotopes. Quaternary 2, 9Paper 310.

Kern, Z., Hatvani, I.G., Czuppon, G., Fórizs, I., Erdélyi, D., Kanduč, T., Palcsu, L., Vreča, P., 2020a. Isotopic 'Altitude' and 'Continental' Effects in Modern Precipitation across the Adriatic–Pannonian Region. Water 12, 1797.

Kern, Z., Erdélyi, D., Vreča, P., Krajcar Bronić, I., Fórizs, I., Kanduč, T., Štrok, M., Palcsu, L., Süveges, M., Czuppon, G., Kohán, B., Gábor Hatvani, I., 2020b. Isoscape of amount-weighted annual mean precipitation tritium (^{3}H) activity from 1976 to 2017 for the Adriatic–Pannonian region – AP3H_v1 database. Earth Syst. Sci. Data 12, 2061–2073.

Kim, S.-T., O'Neil, J.R., 1997. Equilibrium and nonequilibrium oxygen isotope effects in synthetic carbonates. Geochim. Cosmochim. Acta 61, 3461–3475.

Kluge, T., John, C.M., Boch, R., Kele, S., 2018. Assessment of Factors Controlling Clumped Isotopes and δ^{18}O Values of Hydrothermal Vent Calcites. Geochem. Geophys. Geosyst. 19, 1844–1858.

Koltai, G., Spötl, C., Shen, C.-C., Wu, C.-C., Rao, Z., Palcsu, L., Kele, S., Surányi, G., Bárány-Kevei, I., 2017. A penultimate glacial climate record from southern Hungary. J. Quat. Sci. 32, 946–956.

Krajcar Bronić, I., Barešić, J., Borković, D., Sironić, A., Mikelić, I.L., Vreča, P., 2020. Long-Term Isotope Records of Precipitation in Zagreb, Croatia. Water 12, 226.

Meckler, A.N., Ziegler, M., Millán, M.I., Breitenbach, S.F.M., Bernasconi, S.M., 2014. Long-term performance of the Kiel carbonate device with a new correction scheme for clumped isotope measurements. Rapid Commun. Mass Spectrom. 28, 1705–1715.

Meckler, A.N., Affolter, S., Dublyansky, Y.V., Krüger, Y., Vogel, N., Bernasconi, S.M., Frenz, M., Kipfer, R., Leuenberger, M., Spötl, C., Carolin, S., Cobbk, M., Moerman, J., Adkins, J.F., Fleitmann, D., 2015. Glacial-interglacial temperature change in the tropical West Pacific: a comparison of stalagmite-based paleo-thermometers. Quat. Sci. Rev. 127, 90–116.

Meijer, H.A.J., Li, W.J., 1998. The use of electrolysis for accurate δ^{17}O and δ^{18}O isotope measurements in water. Isot. Environ. Health Stud. 34, 349–369.

Müller, I.A., Fernandez, A., Radke, J., van Dijk, J., Bowen, D., Schwieters, J., Bernasconi, S.M., 2017. Carbonate clumped isotope analyses with the long-integration dual-inlet (LIDI) workflow: Scratching at the lower sample weight boundaries. Rapid Commun. Mass Spectrom. 31, 1057–1066.

Petersen, S.V., Defliese, W.F., Saenger, C., Daëron, M., Huntington, K.W., John, C.M., Kelson, J.R., Bernasconi, S.M., Colman, A.S., Kluge, T., Olack, G.A., Schauer, A.J., Bajnai, D., Bonifacie, M., Breitenbach, S.F.M., Fiebig, J., Fernandez, A.B., Henkes, G. A., Hodell, D., Katz, A., Kele, S., Lohmann, K.C., Passey, B.H., Peral, M.Y., Petrizzo, D.A., Rosenheim, B.E., Tripati, A., Venturelli, R., Young, E.D., Winkelstern, I.Z., 2019. Effects of improved ^{17}O correction on interlaboratory agreement in clumped isotope calibrations, estimates of mineral-specific offsets, and temperature dependence of acid digestion fractionation. Geochem. Geophys. Geosyst. 20, 3495–3519.

Piasecki, A., Bernasconi, S.M., Grauel, A.-L., Hannisdal, B., Ho, Sz.L., Leutert, T.J., Marchitto, T.M., Meinicke, N., Tisserand, A., Meckler, N., 2019. Application of Clumped Isotope Thermometry to Benthic Foraminifera. Geochem. Geophys. Geosyst. 20, 2082–2090.

Riechelmann, D.F.C., Deininger, M., Scholz, D., Riechelmann, S., Schröder-Ritzrau, A., Spötl, C., Richter, D.K., Mangini, A., Immenhauser, A., 2013. Disequilibrium carbon and oxygen isotope fractionation in recent cave calcite: Comparison of cave precipitates and model data. Geochim. Cosmochim. Acta 103, 232–244.

Rozanski, K., Araguás-Araguás, L., Gonfiantini, R., 1992. Relation between long-term trends of oxygen-18 isotope composition of precipitation and climate. Science 258, 981–985.

Rozanski, K., Araguás-Araguás, L., Gonfiantini, R., 1993. Isotopic patterns in Global Precipitation. Climate change in continental isotopic records. Geophys. Monogr. Ser. 78, 1–36.

Schmid, T.W., Bernasconi, S.M., 2010. An automated method for "clumped-isotope" measurements on small carbonate samples. Rapid Commun. Mass Spectrom. 24, 1955–1963.

Schwarcz, H.P., Harmon, R.S., Thompson, P., Ford, D.C., 1976. Stable isotope studies of fluid inclusions in speleothems and their paleoclimatic significance. Geochim. Cosmochim. Acta 40, 657–665.

Spratt, R.M., Lisiecki, L.E., 2016. A Late Pleistocene sea level stack. Clim. Past 12, 1079–1092.

Tremaine, D.M., Froelich, P.N., Wang, Y., 2011. Speleothem calcite farmed in situ: Modern calibration of δ^{18}O and δ^{13}C paleoclimate proxies in a continuously-monitored natural cave system. Geochim. Cosmochim. Acta 75, 4929–4950.

Turney, C.S.M., Jones, R.T., 2010. Does the Agulhas current amplify global temperatures during super-interglacials? J. Quat. Sci. 25, 839–843.

Uemura, R., Nakamoto, M., Asami, R., Mishima, S., Gibo, M., Masaka, K., Jin-Ping, C., Wu, C.-C., Chang, Y.-W., Shen, C.-C., 2016. Precise oxygen and hydrogen isotope determination in nanoliter quantities of speleothem inclusion water by cavity ring-down spectroscopic techniques. Geochim. Cosmochim. Ac. 172, 159–176.

Uemura, R., Kina, Y., Shen, C.-C., Omine, K., 2020. Experimental evaluation of oxygen isotopic exchange between inclusion water and host calcite in speleothems. Clim. Past 16, 17–27.

Varsányi, I., Palcsu, L., Kovács, Ó., 2011. Groundwater flow system as an archive of palaeotemperature: Noble gas, radiocarbon, stable isotope and geochemical study in the Pannonian Basin, Hungary. Appl. Geochem. 26, 91–104.

Vodila, G., Palcsu, L., Futó, I., Szántó, Zs, 2011. A 9-year record of stable isotope ratios of precipitation in Eastern Hungary: Implications on isotope hydrology and regional palaeoclimatology. J. Hydrol. 400, 144–153.

Vogel, N., Scheidegger, Y., Brennwald, M.S., Fleitmann, D., Figura, S., Wieler, R., Kipfer, R., 2013. Stalagmite water content as a proxy for drip water supply in tropical and subtropical areas. Clim. Past 9, 1–12.

Watkins, J.M., Hunt, J.D., Ryerson, F.J., DePaolo, D.J., 2014. The influence of temperature, pH, and growth rate on the δ^{18}O composition of inorganically precipitated calcite. Earth Planet. Sci. Lett. 404, 332–343.

Zhang, R., Schwarcz, H.P., Ford, D.C., Serefiddin-Schroeder, F., Beddows, P.A., 2008. Absolute palaeotemperature record from 10 to 6 ka inferred from fluid inclusion D/H ratios of a stalagmite from Vancouver Island. British Columbia. Geochim. Cosmochim. Acta 72, 1014–1026.